Check for updates

Alexander Stolz[1]
Kevin Jooß[1,2]
Oliver Höcker[1,3]
Jennifer Römer[1,4]
Johannes Schlecht[1,5]
Christian Neusüß[1]

[1]Faculty of Chemistry, Aalen University, Aalen, Germany
[2]Research Unit Analytical BioGeoChemistry, Helmholtz Zentrum München, Neuherberg, Germany
[3]Instrumental Analytical Chemistry, University of Duisburg-Essen, Essen, Germany
[4]Institute of Analytical Chemistry, Chemo- and Biosensors, University of Regensburg, Regensburg, Germany
[5]Department of Pharmaceutical/Medicinal Chemistry, Friedrich Schiller University, Jena, Germany

Received August 1, 2018
Revised September 6, 2018
Accepted September 7, 2018

Review

Recent advances in capillary electrophoresis-mass spectrometry: Instrumentation, methodology and applications

Capillary electrophoresis (CE) offers fast and high-resolution separation of charged analytes from small injection volumes. Coupled to mass spectrometry (MS), it represents a powerful analytical technique providing (exact) mass information and enables molecular characterization based on fragmentation. Although hyphenation of CE and MS is not straightforward, much emphasis has been placed on enabling efficient ionization and user-friendly coupling. Though several interfaces are now commercially available, research on more efficient and robust interfacing with nano-electrospray ionization (ESI), matrix-assisted laser desorption/ionization (MALDI) and inductively coupled plasma mass spectrometry (ICP) continues with considerable results. At the same time, CE-MS has been used in many fields, predominantly for the analysis of proteins, peptides and metabolites. This review belongs to a series of regularly published articles, summarizing 248 articles covering the time between June 2016 and May 2018. Latest developments on hyphenation of CE with MS as well as instrumental developments such as two-dimensional separation systems with MS detection are mentioned. Furthermore, applications of various CE-modes including capillary zone electrophoresis (CZE), nonaqueous capillary electrophoresis (NACE), capillary gel electrophoresis (CGE) and capillary isoelectric focusing (CIEF) coupled to MS in biological, pharmaceutical and environmental research are summarized.

Keywords:
Capillary electrophoresis / CE-MS / Mass spectrometry
DOI 10.1002/elps.201800331

1 Introduction

Mass spectrometry (MS) has been successfully coupled to chromatographic separation systems such as gas and liquid chromatography (GC, LC) for a long time and these systems are now considered the 'workhorses' of environmental, clinical and biological analysis. Unlike chromatography, with a separation mechanism based on an equilibrium of analytes between stationary and mobile phase, capillary electrophoresis (CE) offers a non-equilibrium separation mechanism based on different parameters such as charge and hydrodynamic radius (capillary zone electrophoresis (CZE)), isoelectric point (capillary isoelectric focusing (CIEF)) or molecular weight (capillary gel electrophoresis(CGE)) of analytes and therefore, represents an interesting alternative. CE offers the possibility to obtain complementary separation selectivity to commonly performed chromatography and thus enables new solutions for analytical questions, widening the spectrum of accessible analytes. Separation under near-physiological conditions is especially beneficial for biological studies on protein folding, function and interaction. Sample amounts are inherently small, which often is regarded as limitation since

Correspondence: Professor Christian Neusüß, Beethovenstraße 1, 73430 Aalen, Germany
E-mail: eusuess@hs-aalen.de

Abbreviations: **ADC**, antibody-drug-conjugate; **ALS**, alternating least square; **APTS**, 8-aminopyren-1,3,6-trisulfonate; **CITP**, capillary isotachophoresis; **CKD**, chronic kidney disease; **CSF**, cerebrospinal fluid; **DMA**, *N,N*-dimethylacetamide; **EACA**, epsilon-aminocaproic acid; **FQ**, fluoroquinolone; **GAG**, glycosaminoglycan; **HA**, hyaluronic acid; **HCP**, host cell proteins; **HMT**, Human Metabolome Technologies; **IAE**, immunoaffinity extraction; **iCIEF**, imaging capillary isoelectric focusing; **ID**, identity; **IM**, ion mobility; **IMAC**, immobilized metal ion affinity chromatography; **MCR**, multivariate curve resolution; **miRNA**, micro ribonucleic acid; **MSI**, multi-segment injection; **NOM**, Natural organic matter; **NP**, nanoparticle; **ppb**, parts per billion; **ppt**, parts per trillion; **PSA**, prostate specific antigen; **PWEAB**, photolithography-wet etching-anodic-bonding; **REPSM**, reversed electrode polarity stacking mode; **SCX**, strong cation exchange; **SL**, sheath liquid; **SLE**, selective laser induced etching; **SP**, single particle; **TG2**, human tissue transglutaminase; **TQ**, triple quadrupole; **UHPLC**, ultra-high performance liquid chromatography; **UV**, ultraviolet

Color online: See the article online to view Figs. 1–7 in color.

© 2018 WILEY-VCH Verlag GmbH & Co. KGaA, Weinheim

concentration sensitivity is hampered. However, it offers great potential for the analysis of volume-restricted and precious samples. On the other hand, mass spectrometry is the key technology for fast and detailed characterization of small and large analytes based on mass and fragmentation pattern and is especially powerful when combined with efficient separation.

These facts have led to an ever-increasing interest in CE-MS applications in various analytical fields. This development is further supported by major analytical instrument manufacturers, providing commercially available interfaces to hyphenate CE with MS. In the past, research was mainly focused on the development of novel and optimized instrumentation to enable efficient CE-MS interfacing [1] and optimizations toward MS-compatibility of various methods such as ITP-preconcentration, chiral separation and methods using surfactants [2]. With the development of more powerful and user-friendly methodologies, research on CE-MS is now developing toward evaluating applications in environmental, pharmaceutical, clinical and especially biological and biochemical research as an interesting alternative to commonly used analytical platforms.

This review provides an overview of major instrumental and applicative developments regarding CE-MS published between June 2016 and May 2018. This includes instrumentation regarding coupling of different CE separation principles (CZE, NACE, CGE, CIEF, ITP) with mass spectrometry, including different ion sources (ESI, MALDI, ICP) and the development of multidimensional separation platforms, as well as recent applications of CE-MS in various analytical fields. This article belongs to a series of regularly published articles and represents a continuation of the latest review in this series by Týčová et al. [2]. Due to the vast number of publications using chip-based electrophoretic separations, these are not covered here and specific reviews to recent developments on this subject are available elsewhere [3, 4]. Techniques based on chromatographic effects such as CEC and MEKC are also not covered in this review. To get a better overview about separation platforms and interfaces, each section is accompanied with a table, summarizing methods and applications of the publications relevant to the respective field.

2 Instrumentation, interfacing, methodology

2.1 CE-ESI-MS interfacing

ESI is the method of choice, when mass spectrometry is used for online characterization of organic ionic molecules after separation by capillary-based electromigration techniques. The coupling of CE to ESI-MS remains a challenging task since many requirements need to be fulfilled for stable operation. These include mainly the drain of the current generated by the applied separation voltage and, in most cases, the electrospray voltage as a second independent circuit as well as consideration of electroosmotic flow and magnitude. General instrumental aspects of CE-MS hyphenation were covered in previous reviews [5, 6] and are not discussed here in detail. The co-axial sheath liquid interface with high sheath liquid flow rates of 2 to 10 μL/min is still the standard interface for robust and high throughput analyses as demonstrated by the vast majority of application-focused publications. However, substantial dilution of the CE effluent leads to low ionization efficiency. New developments aim for the improvement of sensitivity while trying to keep flexibility, robustness and ease of use. The inherently low flow rates of CE (0–100 nL/min) are considered to be beneficial to reduce ion suppression and improve ionization efficiency by miniaturization of all related parts, resulting in the formation of smaller droplets. While some approaches try to enable the use of standard separation capillaries for reasons of flexibility and ease of use, others aim for maximum efficiency which may cause difficulties in handling, due to fragile parts and limitations for the separation. The following section describes a selected variety of innovations published in recent years.

2.1.1 Sheathless interfaces

Sheathless interfaces are most intuitive in construction since the separation buffer is the only liquid involved and no dilution occurs, but realizing a proper and long term stable electrical contact is challenging. The opportunity for post-separation modification is also limited, compromising separation and electrospray conditions. In recent years, several sheathless interfaces used cracks in the capillary wall as an alternative to the sheathless porous tip interface introduced in 2007 [7] to obtain a robust tip geometry while simultaneously enabling full grounding of the capillary.

Nguyen et al. [8] showed a simple way for the fabrication of a sheathless interface with a sub-micrometer fracture in the last 1.5 cm of the separation capillary and etched spray tip with a wall thickness of 10–20 μm. After removal of the polyimide coating, the capillary was inserted into a PTFE shrink tubing and a crack was made with an optical fiber cleaver which penetrates the PTFE tubing to enable electrical contact while keeping mechanical stability. Afterward a PMMA reservoir filled with buffer solution was attached by gluing with an electrode for electrical contact (Fig. 1A). In the experiments, separation currents of 20 μA were obtained with a possible maximum of 300 μA. Different coatings for the analysis of tryptic BSA peptides and proteins such as insulin, tissue factor, α-synuclein, and ubiquitin showed the versatility for various potential applications.

Johnson et al. showed an alternative way to realize electrical contact by several precise CO_2 laser ablations (25 μm diameter) of the capillary wall close to the beveled spray tip, to create a large surface area. [9]. A cast of cellulose acetate dissolved in acetone was applied afterward to both, stabilize the capillary mechanically and to serve as electrical contact by transport of small ions to the electrode (Fig. 1B). This can also be used for post-separation pH modifi-

© 2018 WILEY-VCH Verlag GmbH & Co. KGaA, Weinheim

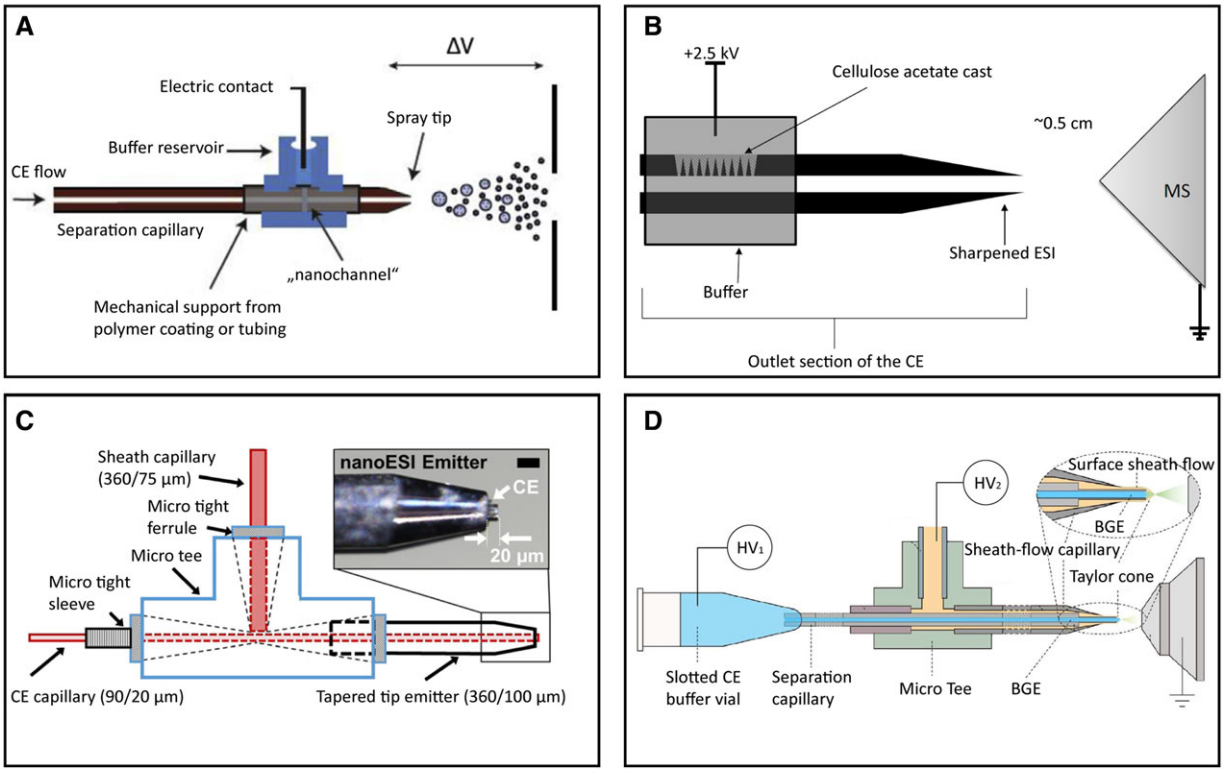


Figure 1. Schematics of (A) Sheathless interface with nanochannel, adapted from [8]. Copyright © 2016, with permission from Elsevier; (B) Sheathless interface with 24 holes using laser ablation with cellulose acetate, adapted by permission from Springer Nature [9], Copyright © 2017. (C) Tapered tip sheath liquid interface, adapted by permission from Springer Nature [21], Copyright © 2016; (D) Sheath flow interface with extendable separation capillary, adapted from [23]. Copyright © 2018, with permission from Elsevier.

cation by changing the pH value in the interface reservoir. While these capillaries could be manufactured automated, non-aqueous electrolytes might be critical for their long-term stability.

In a similar approach, Hirayama et al. applied a microdialysis membrane attached to a polymer plate with a hole and to a capillary approximately 2 mm away from the emitter tip, stabilized it with cyanoacrylate glue and created a small crack with a diamond cutter [10]. This interface was applied for non-targeted metabolome analysis of human cancer cells and compared to the standard co-axial sheath liquid interface, increased the number of identified peaks by a factor of 2.5.

Týčová et al. applied their so-called 'interface-free' sheathless nanospray instrumentation to blood plasma samples with small improvements over their previous version [11], such as a hydrophobic coating at the grinded tip [12]. For this hyphenation, in its simplest form, only one power supply for separation and electrospray voltage with no additional grounding is needed. It uses 15 µm id capillaries with 30 kV and 3.5 µA separation current, which is drained by the MS inlet. The small id, low flow rate and lack of sheath liquid may enable high ionization efficiencies and the use of only one capillary without additional parts make the interface user friendly. However, this setup is limited regarding applicable capillary diameters, furthermore separation and MS detection cannot be performed simultaneously in the actual set-up.

To enable post-separation chemistry, Kammeijer et al. modified the commercialized version of the sheathless porous tip CESI system (Sciex) with an in-house built cone to introduce a dopant enriched nitrogen gas coaxially around the porous etched capillary tip to enhance ionization efficiency and sampling by a guided electrospray plume [13]. A detailed characterization of the behavior depending on gas flow, type of dopant and concentration for the analysis of different glycopeptides was performed with the result of an overall improved ionization efficiency compared to the conventional setup. The determined LODs were significantly lower compared to a nanoLC-MS system. These results are promising for all fields of application where post column chemistry can be beneficial, such as addition of pH-modifiers or supercharging agents.

Jarvas et al. applied the CESI 8000 with porous tip sheathless interface for the direct infusion of a monoclonal antibody solution and investigated the effect of different flow rates on the sensitivity and ion suppression of a saccharide in presence of a peptide, known to cause interference [14]. Below flow rates of 50 nL/min, ion suppression was reduced, demonstrating the benefits of low flow rates. In another article, Javas et al. evaluated the performance of separation systems for

© 2018 WILEY-VCH Verlag GmbH & Co. KGaA, Weinheim

analysis of strongly negative charged analytes in reversed polarity mode with counter EOF, which is especially of interest for the use of sheathless interfaces [15]. Since a flow toward the ion source of the MS is necessary for sheathless systems, an inlet pressure is needed to maintain electrospray. Computational simulations and experiments determined a theoretical plate number of N∼950,000/m in presence of a counter EOF without inlet pressure compared to N∼480,000/m with applied inlet pressure, which appears to be sufficient for the 8-aminopyren-1,3,6-trisulfonate (APTS)-labeled glycans used in the experiments.

2.1.2 Nanoflow sheath liquid interfaces

Most interfaces accomplish the electrical contact over a sheath liquid (SL), which also offers more possibilities to manipulate the electrospray process, since it is decoupled from the separation conditions.

Sarver et al. modified the nanoSL interface developed by Dovichis group [16] (commercialized by CMP Scientific) in order to perform ESI in negative ionization mode [17]. They obtained stable spray conditions by using 10 mM ammonium acetate in 70% methanol as sheath liquid and coating of the emitter with 3-aminopropyltrimethoxysilane to reverse the EOF in the used glass emitter. However, recent calculations and measurements indicate that the EOF is not the driving force in this type of interface and rather the sheath liquid is important to obtain stable spray conditions [18].

González-Ruiz et al. further improved their user friendly and robust nano-flow sheath liquid interface [19], that uses a blunt metal needle serving as sheath flow capillary with a separation capillary protruding the needle by ∼200 μm. The new approach reduces the capillary and needle od to 150 and 360 μm, respectively, which enables lower sheath liquid flow rates between 300 nL/min and 2 μL/min with a nanoflow pump [20]. A technical solution was presented to use smaller od capillaries in a commercial CE-instrument. To minimize mixing effects and thus peak broadening, residence time in the Taylor cone should be short. The new design reduces the Taylor cone volume from 125 to 9 nL, simultaneously reducing residence time of the analytes. The interface was applied to neural cell culture samples for neurotransmitter and metabolome analysis.

A similar co-axial setup was used by Choi et al. for bottom-up proteomics of a mouse cortex, using a 20 μm id and 90 μm od fused silica capillary protruding a metal needle (100 μm id and 360 μm od, tapered to ∼100 μm od) with a defined sheath liquid flow between 200 and 350 nL/min [21] (Fig. 1C). Compared with a previous design of the same group [22], the new interface exhibits a ∼100 fL Taylor cone volume at 300 nL/min sheath liquid flow and reaches a ∼70-fold higher sensitivity.

Fang et al. designed an interesting approach for a nanoflow sheath liquid interface with an extendable tip, featuring a so-called surface flow [23]. The separation capillary with a 20 μm id is chemically etched to reduce the od to 30 μm and is introduced into a tapered sheath flow capillary made of glass with 35 μm id and 40 μm od (Fig. 1D). After optimization, the separation capillary protrudes by approximately 200 μm from the outer capillary and serves as the electrospray emitter. The sheath liquid is driven by a syringe pump and flows on the surface of the separation capillary and mixes with the separation effluent inside the Taylor cone with a volume of 4 pL, using flow rates of 200 nL/min. Extension of the tip showed improved sensitivity when compared to the assembly with retracted tip. The interface was applied for the analysis of a peptide mixture, showing good repeatability for peak intensity and spray stability. While this interface might offer great sensitivity due to its small dimensions with minimum dead volume and low sheath liquid flows, it is difficult to be manufactured compared to others.

Whereas the handling of novel interfacing techniques can be assessed, it is difficult to estimate its analytical performance. The determination of LODs strongly depends on factors such as analytes, buffer systems and instrumental performance. The definition of absolute, molar LODs further complicates comparability since the low injection volumes in CE generally results in low molecular LODs even for modest concentration sensitivity. To address this issue, Höcker et al. attempted a systematic comparison of a nanoflow sheath liquid interface to a sheathless porous tip interface and the standard co-axial sheath liquid interface under optimized conditions for organic acids, peptides and a reduced monoclonal antibody, demonstrating a similar range of intensity and peak area enhancement for both nanoflow approaches (improvement factors 13-114) [18].

2.1.3 Instrumental amendments: CE equipment and additional detectors

Besides the development of improved interfaces, additional progresses were made in instrumentation to overcome common problems in CE-MS. Flaherty et al. characterized a modified high voltage power supply, providing the ESI voltage after CE separation. The drain of the high currents in CE makes the device useful at higher currents compared to standard devices [24]. ESI-MS can be accompanied by other detectors such as UV/VIS or capacitively coupled contactless conductivity detectors (C^4D), enabling an additional selectivity in detection. Beutner et al. applied both, C^4D and ESI-MS detection in nonaqueous capillary electrophoresis (NACE), which is especially suited due to the low conductivity of BGE in NACE [25]. They showed complementary detection in mixtures of organic and inorganic ions, where the latter can be detected by the C^4D detector. C^4D prior to MS detection is also of interest to characterize the CE-MS interface in terms of peak broadening caused by the MS-hyphenation. Two C^4D detectors were recently combined to determine the correct mobility and EOF prior to MS detection [26]. Moreover, for volatile analytes C^4D can be more sensitive than ESI-MS.

© 2018 WILEY-VCH Verlag GmbH & Co. KGaA, Weinheim

2.2 CE-MS interfacing with other ionization methods

Though ESI is the most commonly applied ionization technique considering CE-MS coupling, there are interfaces utilizing different types of ionization. The following paragraph is predominantly dedicated to new technical developments regarding alternative ionization techniques. Applications of these coupling are mentioned in the following sections.

Matrix assisted laser desorption/ionization (MALDI) is well known for being more tolerant against non-volatile electrolyte components compared to ESI, which can be beneficial. In this regard, offline hyphenation of CE with MALDI-MS enables the possibility for additional sample treatment, including enrichment steps or enzymatic digestion. In the past years, efforts have been dedicated especially to the automation of CE-MALDI-MS setups. Based on the first fully automated offline interface introduced in 2014 [27], Biacchi et al. developed a CE-MALDI-MS/MS system for the top- and middle-down analysis of monoclonal antibodies (mAbs), which enables sample enrichment by multiple spotting [28]. In this work, it could be shown that the enrichment step is required to achieve sufficient sensitivity for top-down analysis. A very interesting approach for single-cell analysis was developed by the Sweedler group. First, optically guided MALDI-MS is performed followed by liquid micro-junction extraction and subsequent CE-ESI-MS analysis [29]. With this semi-automated setup, the benefits of both ionization techniques could be utilized covering a broad range of analytes.

CE hyphenated to inductively coupled plasma (ICP) mass spectrometry is routinely applied for (trace) elemental analysis and commercial interfaces are available. Still, there is room for improvement, especially regarding the interface design (nebulization and transport efficiency). In general, three types of CE-ICP-MS interfaces are applied: sheath flow (i), sheathless (ii) and hybrid generation interfaces (iii). Among these three types, sheath flow interfaces are most frequently used. A home-built sheath flow interface was developed by Yang et al. [30]. This interface prevents the suction effect caused by the ICP-MS system by means of two individual peristaltic pumps and a tee-union. In this way, improved resolution and close to zero dead volume could be achieved. Based on their previous results, the same group improved interface settings for the quantification of zinc-based fungicides by CZE-ICP-MS [31]. An alternative interface concept was introduced by Shuai et al. [32]. Here, the standard microconcentric nebulizer (200–400 μL/min) was replaced by a polyfluoroalkoxy nebulizer (10–20 μL/min), thus reducing dead volumes, dilution effects and improving overall nebulization. Furthermore, a quadrupole ion deflector decreased the interference caused by sample matrix. Due to poor injection repeatability, CE is often associated with low precision considering drifts in migration time and peak area. Thus, Holtkamp et al. evaluated Co(III)-complexes as versatile internal standards for CE-ICP-MS, testing a wide range of potential BGEs (pH 2.8–9.0) [33] . These complexes are stable and useful at different pH of BGE and not only in CE-ICP-MS, but also for UV and ESI-MS detection. Furthermore, Cheng et al. counteracted the limited injection volume of CE by implementing a multichannel (2–20 array) microchip directly to ICP-MS with a sheath flow interface, improving the sensitivity for trace elemental analysis reaching lower ppt range for mercury species [34]. In addition, they aspire to apply a sheathless interface in the future to further improve the sensitivity of the homebuilt design.

Chaudhari et al. presented the coupling of CGE to time-of-flight mass spectrometry in hollow nanomechanical resonators [35]. Such a system allows the rough mass determination of proteins in a small portable instrument since it does not require vacuum. In addition, ambient ionization techniques have been applied for CE-MS coupling. Zhang et al. developed a CE-MS interface based on dielectric barrier discharge ionization, separating a mixture of metronidazole and acetaminophen solutions in a proof-of-concept study [36].

2.3 New developments in multidimensional separations

An ever-increasing demand of analytical techniques capable of handling samples with complex matrices and/or detecting many different compounds in a single run has led to the development of multidimensional separation techniques. The introduction of a second dimension, ideally with a high degree of orthogonality to the first, offers the opportunity to enhance separation efficiency. Additionally, this enables the use of CE separation methods with ESI-incompatible electrolytes in the first dimension. Intense research has been devoted to the development of online two-dimensional chromatographic separation systems. However, two-dimensional capillary electrophoresis is not as straight forward as utilizing two-dimensional gas or liquid chromatography due to the challenge of high voltage handling and volume transfer in the nanoliter range. Thus, efficient 2D-interfacing for online 2D-separations of capillary electromigration methods is a rather new field of research. This chapter focuses on the development of online-multidimensional separation techniques; offline-coupling is not considered in this section and according publications are mentioned later in this review.

Sydes et al. introduced a novel microfluidic interface manufactured by selective laser induced etching (SLE) and compared it to a microchip obtained via classical photolithography-wet etching-anodic-bonding (PWEAB) and a classical capillary as reference [37]. To compare the interfaces, they used a one-dimensional separation of the amino acids arginine and lysine as model. Improvements in peak shape and migration time could be observed using the SLE-chip.

In a previous study, our group introduced an interface based on a mechanical four-port valve with a nanoliter sample loop [38]. One of the first application of the valve interface was CIEF-CZE-MS coupling [39]. Proteins were separated by CIEF according to their pI values. Selected fractions were transferred to the second dimension where the ESI-interfering ampholytes were segregated from the protein of interest by

© 2018 WILEY-VCH Verlag GmbH & Co. KGaA, Weinheim

CZE. The same analytical platform was successfully applied for multiple heart-cut analysis of a protein mix and charge variants of a deglycosylated model antibody [40]. This separation platform was further extended by hyphenation of imaging CIEF (iCIEF) with CZE in the second dimension [41]. Further applications include the separation of charge variants of deglycosylated trastuzumab [42], and the quantification of ascorbic acid, acetylsalicylic acid and degradation product in effervescent tablets by utilizing tricine as BGE [43]. Applications are described in more detail in the different parts of Section 3. Altogether, these approaches demonstrate the four-port valve as a universal interface for online hyphenation of CE and MS-incompatible methods.

3 Analytical applications

3.1 Protein analysis and proteomics

CE-MS is widely used in the field of bottom-up and top-down proteomics. Conventional one-dimensional CE-MS as well as multidimensional separation platforms, including at least one CE dimension were applied for the analysis of intact and digested proteins in recent publications.

3.1.1 Intact protein analysis and top-down proteomics

CE has been extensively used for the separation of intact proteins. Compared to LC-based methods, CE usually exhibits a different selectivity, often leading to a better separation efficiency for intact proteins. Thus, intense research is conducted on the development of new methodologies for intact protein separation and CE-MS based top-down proteomics.

Since separation can be performed under near physiological conditions, CE was recently applied for the separation of protein conformers. Bertoletti et al. evaluated the capabilities of CE-MS for the separation and identification of protein conformers using β_2-microglubulin as model compound. They were able to separate two conformers and concluded that a sheathless interface is best suited to maintain conformational integrity after ionization [44]. Another study demonstrated the identification of several conformers of antithrombin based on their different charge-state-distributions [45]. Belov et al. presented a CE-MS method for the native separation of proteins and protein complexes. The comparison of uncoated with polyacrylamide-coated capillaries showed a better reproducibility and efficiency for the latter. After initial method development with model proteins, the platform was applied to characterize a mAb and subsequently an *E. coli* ribosomal isolate. 200 proteoforms of 51 proteins were identified under native conditions with additional identification of noncovalent protein complexes [46]. Mirnov et al. developed a CE-UV-IM-MS method for the simultaneous analysis of structure and activity of the model enzyme human tissue transglutaminase (TG2) in a single run [47]. For all kinetic experiments, TG2 was incubated with a mixture of two substrates and subsequently analyzed. The CE separation resulted in two peaks with the same mass as determined by MS but different cross-sections, thus indicating the presence of two conformers. Relative quantification of the protein conformers was based on UV detection, whereas MS was used to semi-quantify substrate and product of the enzymatic reaction to calculate the activity of TG2. The same workflow was also applied for calculation of inhibitor kinetics. By combining the conformational and activity data, the authors concluded that inhibition locks the enzyme in a conformational state, thus indicating that only one of the conformers shows notable enzymatic activity. Han et al. coupled immunoaffinity capture with CE-MS to determine absorption, distribution, metabolism, and excretion figures of a wild type and sequence engineered Fc fragment from mice serum after in vivo administration [48].

Tengattini et al. used CZE-MS for the intact characterization of synthetically produced glycoconjugate vaccines [49]. The influence of the reaction conditions on the stability of the carrier proteins was evaluated. They were able to separate and identify truncated, oxidized and even deamidated forms. CZE-MS was successfully applied for top-down characterization of the *E. coli* proteome [50]. By combining an optimized separation method with a dynamic pH junction stacking method, injection of up to 1 μL sample was possible and resulted in the identification of 600 proteoforms of 200 proteins.

SDS is often used in sample preparation and treatment of proteins and can be disturbing in mass spectrometry. An in-capillary strategy was developed by Sánchez-Hernández for decomplexing protein-SDS complexes. Here, the co-injection of positively charged surfactants (cetyltrimethylammonium bromide or benzalkonium chloride) and methanol as organic solvent lead to recoveries of MS peak intensities up to 97 and 95% compared to SDS-free protein samples of the same concentration [51].

All previously mentioned studies applied CZE for protein separation. Although CIEF offers high resolution in protein separation, its application in systems with mass spectrometric detection is still scarce. This fact may be attributed to the two-step procedure comprising focusing and mobilization and the usage of highly-ESI interfering ampholytes. Zhu et al. presented a simple method for chemical mobilization in CIEF-MS by injecting a rather short zone of ammonia solution acting as catholyte prior to sample/ampholyte injection [52]. Chemical mobilization started when the acidic sheath liquid neutralized the ammonia solution. Páger et al. developed a CIEF-MS method applying narrow range ampholytes by sequential injection [53]. They showed that this sequential injection protocol enabled the detection of CIEF-separated proteins.

3.1.2 Bottom-up proteomics

Although top-down applications are increasing in recent publications, bottom-up proteomics is still state-of-the-art and

© 2018 WILEY-VCH Verlag GmbH & Co. KGaA, Weinheim

more commonly applied. CE offers high separation efficiency for proteolytic peptides and was thus applied for a variety of bottom-up methodologies.

Dada's group presented an optimized CZE-MS method for the separation of peptides of therapeutic proteins [54]. The addition of either of two organic additives, *N,N*-dimethylacetamide (DMA) or *N,N*-dimethylformamide (DMF) to the BGE improved the separation of peptides of a recombinant mAb after digestion with Lys-C, compared to a 10% acetic acid BGE. The authors attributed the enhanced performance to an altered proteolytic equilibrium of the peptides by the dipolar organic additives. In a subsequent study, the same group applied the optimized method to the peptide mapping of a Lys-C-digested antibody-drug-conjugate (ADC) [55]. Chen et al. compared UHPLC-MS with CZE-MS of a bovine lactoferrin digest. They reported that their CZE-method is beneficial for the detection of peptides with high size-to-charge ratios [56]. Reich et al. applied CZE-MS to identify potential protein markers for retinal vein occlusion [57].

Sequential injection of samples can increase the throughput of CE-MS by lowering dead times between runs. Boley et al. showed a doubling in the peptide identification rate [58]. Using such an approach in an offline two-dimensional RPLC-CZE-MS system, Faserl et al. identified 62 000 peptides, representing 6100 proteins in a 12.5 h run by sequential injection of RPLC fractions every 10 min [59]. Peptides could be traced back to the respective LC-fraction by monitoring their charge state. The appearance of peptides with decreasing charge states is repeated for every injected fraction. Figure 2 shows a plot, where identified peptides are represented by different colored dots, depending on the peptide charge state.

Preconcentration and/or clean-up methods are often crucial for the identification of low-abundance proteins. Zhang et al. developed an in-line SPE-CE-MS system for the analysis of protein digests [60]. Up to 11 μL could be loaded, eluted with ammonium hydrogen carbonate solution and separated in acetic acid BGE. 365 peptides were identified from a 1 μg/mL *E. coli*-digest. Chen et al. were able to inject 0.5 μL corresponding to 12% of the available sample by dynamic pH junction sample stacking, enabling a peak capacity of about 380 [61].

Analysis of post-translational modifications (PTMs) is still one of the most ambitious tasks in protein analysis with phosphorylation and deamidation being amongst the most challenging PTMs on commonly used RPLC separation systems. The applicability of CZE-MS for PTM analysis, especially concerning deamidation was demonstrated in recent studies [62–65]. Faserl et al. successfully applied CE-MS for the analysis of the phosphoproteome of PC-12 pheochromocytoma cells. They were able to identify 5686 phosphopeptides after digestion and phosphopeptide enrichment by immobilized metal ion affinity chromatography (IMAC) [65].

In most bottom-up proteomic approaches, peptide identification is based on exact mass and MS/MS spectrum by comparison with comprehensive databases. Although this approach proofed to be powerful, it would be desirable to additionally use retention/migration times to further boost the confidence in peptide identification. Therefore, Krokhin et al. used large-scale bottom-up CE-MS datasets to develop a prediction model for the electrophoretic mobility of peptides based on sequence-specific parameters [66]. The model reached a correlation of $R^2 \sim 0.995$ for predicted versus experimental migration times, indicating a more precise prediction than current RPLC prediction models, which, according to the authors, can be explained by a relative simple separation process of CZE compared to RPLC.

Gusenkov et al. demonstrated the potential of combining a top-down and a bottom-up strategy in a complementary manner [67]. The birch pollen allergen Bet v 1a was nitrated with peroxynitrite which resulted in the formation of nitrotyrosine residues, known to be responsible for an enhanced allergenicity. In a top-down approach, six singly- and doubly-modified proteoforms with different modification sites could be separated. Due to insufficient sequence coverage however, comprehensive nitration analysis was not possible. By combination with a bottom-up approach, most of the nitration sites in the protein could be identified, and nitration propensity could be evaluated.

3.1.3 Multidimensional methods based on fraction collection

Although these studies demonstrate the general application of CZE-MS for the separation and identification of proteolytic peptides, separation performance is often not sufficient to analyze complex samples containing many different proteins and proteoforms. Consequently, the application of multidimensional, offline separation techniques, applying fraction collection prior to CZE-MS detection is gaining popularity in the field of bottom-up proteomics.

Yan et al. employed RPLC pre-fractioning prior to CZE-MS for the separation of a *Xenopus laevis* fertilized egg digest. This two-dimensional offline coupling enabled the identification of 4100 proteins based on 22 000 peptide IDs [68]. Chen et al. used a similar approach, but additionally added a strong cation exchange (SCX) dimension prior to RPLC fractioning, resulting in a three-dimensional separation platform (Fig. 3). This platform was successfully applied for the separation of peptides from a mouse brain digest with 8200 protein identifications based on 65 000 unique peptide IDs. The authors stated that this was the largest bottom-up proteomic dataset using CZE-MS at that time [69]. The group used a similar platform, replacing SCX with SEC for top-down proteomics of the *E. coli* proteome. They were able to identify 5700 proteoforms by SEC-RPLC pre-fractioning combined with CZE-MS [70].

3.2 Monoclonal antibodies

During the past decade, biotechnologically manufactured mAbs have become increasingly important in the treatment of cancer and autoimmune diseases. In this context, a

© 2018 WILEY-VCH Verlag GmbH & Co. KGaA, Weinheim

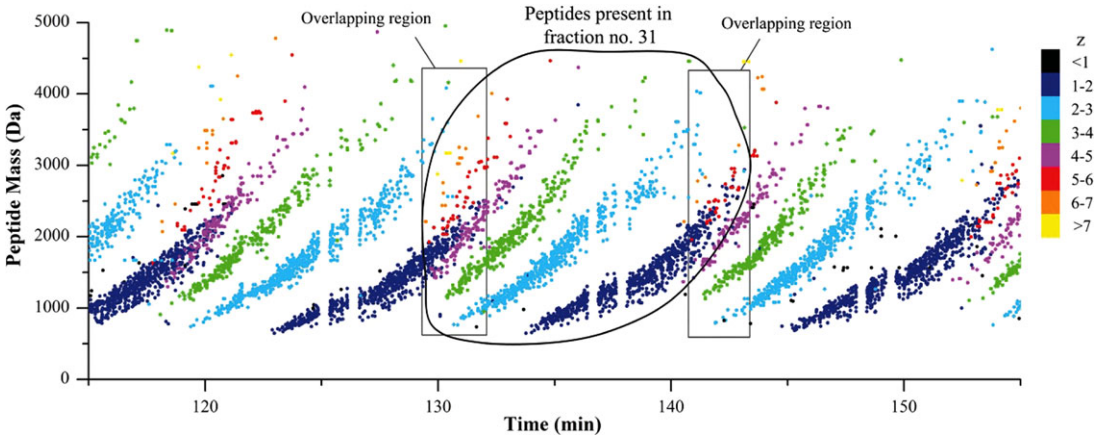


Figure 2. Peptide assignment to an RPLC fraction based on charge state (pH 2.0) in a sequential injection CZE-MS approach. Each dot represents an identified peptide. Peptides assigned to fraction 31 are marked by a cycle. Reprinted from [59] with permission from Wiley. Copyright © 2018 WILEY-VCH.

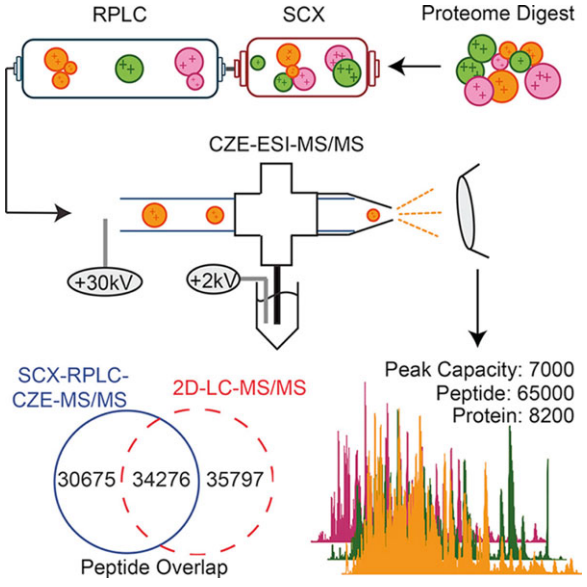


Figure 3. Protein identification by SCX-RPLC-CZE-MS. A mouse brain digest was used as sample. Three salt steps with further RPLC-fraction collection was employed, resulting in 60 fractions analyzed by CZE-MS. This resulted in the identification of 8200 proteins based on 65 000 peptide IDs. Reprinted from [69]. Copyright © 2018, with permission of Elsevier.

detailed characterization of these complex molecules is essential and thus, there is a high demand for appropriate analytical methods. Gahoual et al. recently reviewed the characterization of monoclonal antibodies and related products by CE including CE-MS applications [71]. They highlighted the technical challenges of CE-MS and the main methodologies such as peptide mapping, glycosylation analysis, middle-up and intact analysis for the characterization of mAbs. MAbs are produced in host cells, which may cause contamination by host cell proteins (HCP). Due to a potential effect on safety, efficacy, immunogenicity or stability of the product, identification and quantification of HCPs is necessary. Zhang et al. presented an evaluation of bottom-up proteomic analysis of both HCP digests with and without depleted antibodies by UHPLC-MS, CZE-MS and SCX-SPE-CZE-MS with an online pH gradient elution. [72]. They reported a clear influence of the mAb depletion procedure on peptide identification. Furthermore, a considerable difference was observed, comparing single-shot vs. pH-gradient fractionating analysis after non-depletion and a complementarity between the two methods was suggested. Biacchi et al. reported a proof of principle for a top-down characterization of intact proteins (cytochrome c, lysozyme, RNAse A) and middle-down characterization of cetuximab Fc/2 charge variants using an earlier introduced offline CE-UV/MALDI-MS interface with sample enrichment. [28]. They reported sequence coverages of 17, 14, 20 and 9% corresponding to cytochrome c, lysozyme, RNAse A and cetuximab Fc/2, respectively.

The generic CE methods used in the pharmaceutical industry provide highly selective and efficient separations, but often rely on MS-interfering electrolyte compounds and cannot be coupled directly to MS. As mentioned above, our group developed a two-dimensional CE setup, utilizing a four-port valve. In a heart-cut approach, the main form and two acidic variants of the deglycosylated mAb trastuzumab were separated in a generic but highly ESI-interfering ε-aminocaproic acid (EACA) containing BGE (first dimension), transferred into the second dimension and subsequently detected by MS after the ESI-interfering components were separated [42]. Hence, precise mass data of intact charge variants of trastuzumab including two deamidation products were obtained. In another publication, the separation and mass spectrometric characterization of a model antibody (mAb X) by CIEF-CZE-MS using the same setup was shown [40]. Two CIEF-separated proteoforms of deglycosylated mAb X were transferred into the second dimension in a multiple heart-cut approach and detected by MS. The obtained mass differences in combination with a shift in the p*I* value could be assigned to possible deamidation products. In addition, the described setup was extended to iCIEF-CZE-MS [41]. Due

© 2018 WILEY-VCH Verlag GmbH & Co. KGaA, Weinheim

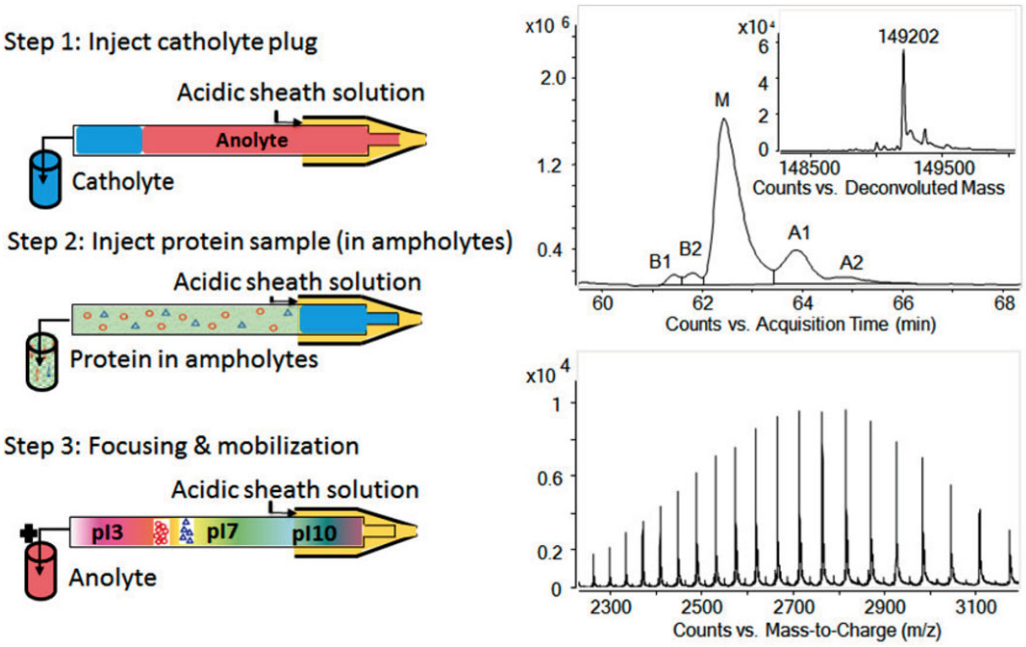


Figure 4. A new online CIEF-MS method for mAb charge variant analysis was developed, including optimization of critical parameters such as MS-compatible anolyte and catholyte, glycerol enhanced sample mixture, ampholyte concentration, and sheath liquid composition. Charge variant profiles of four therapeutic mAbs were obtained and substantiated by imaged iCIEF-UV analyses [73]. Copyright © 2018 American Chemical Society.

to a larger injection volume applicable to the iCIEF system, low-abundance basic variants of stressed trastuzumab could be characterized. Dai et al. reported a CIEF-MS application for the separation and characterization of mAb charge variants [73] as can be seen in Fig. 4. The addition of 15-20% glycerol to catholyte, anolyte and sample solutions in the CIEF-MS approach yielded well-correlating results between CIEF-MS and iCIEF-UV for the four intact therapeutic mAbs bevacizumab, trastuzumab, infliximab and cetuximab. The concentration of 1.5% carrier ampholyte (Pharmalyte 3-10) and the use of a sheath liquid nanospray provides a compromise between CIEF resolution and sensitive MS detection.

3.3 Glycopeptides, glycans and saccharides

Except for glycans containing charged sugar units such as *N*-acetylneuraminic acid, most carbohydrates are uncharged, which complicates their analysis by CE. The introduction of labeling agents such as APTS not only made efficient CE separations accessible, but also enabled sensitive laser-induced fluorescence (LIF) detection. Besides migration time index and the application of glycan standards and/or exoglycosidases, CE-MS methods have been established to facilitate structural identification, especially for unknown glycan structures and in complex samples. In this regard, a CZE-MS method was developed by Varadi et al. using $^{12/13}C_6$ stable isotopologues of 2-aminobenzoic acid as labeling agents [74]. In this way, precise relative quantitative data on mAb glycosylation profiles could be achieved in a twoplex manner, including the batch-to-batch variation of Cetuximab. Snyder et al. developed a sheathless CE-MS method, identifying 77 potential *N*-glycan structures in human serum [75].

In the past, characterization on the glycopeptide level has been commonly performed by RPLC-based methods. Hence, separation is predominantly driven by the hydrophobicity of the peptide and thus, the glycan itself shows only minor influence. In contrast, CE separations based on differences in charge-to-size ratio, can be strongly influenced by the nature of the attached glycan. Consequently, CE represents a promising alternative for glycopeptide separation. In this regard, Kammeijer et al. developed a CZE-ESI-MS method for glycopeptide analysis, including the separation of glycopeptides exhibiting different sialic acid linkages [76]. The applicability of this platform was demonstrated by the analysis of *N*-glycopeptides derived from prostate specific antigen (PSA), detecting 75 different glycopeptides attributed to one single *N*-linked glycosylation site. This impressive separation power is illustrated in Fig. 5. Later, a glycosylation assay for PSA analysis in urine was developed by the same group, based on a similar CE method in combination with dopant (ACN) enriched nitrogen gas to enhance sensitivity [77]. In addition, the Dovichi group observed an improved resolution of different *N*-glycopeptide species with the same peptide sequence, especially if differentially sialylated, compared to RPLC [78]. In a subsequent study, the same group demonstrated an offline RPLC-CZE-ESI-MS method, including RPLC fraction collection with subsequent CZE-ESI-MS analysis [79]. In this way, 268 site-specific *N*-glycopeptides of α-1-acid glycoprotein could be identified, which represented

© 2018 WILEY-VCH Verlag GmbH & Co. KGaA, Weinheim

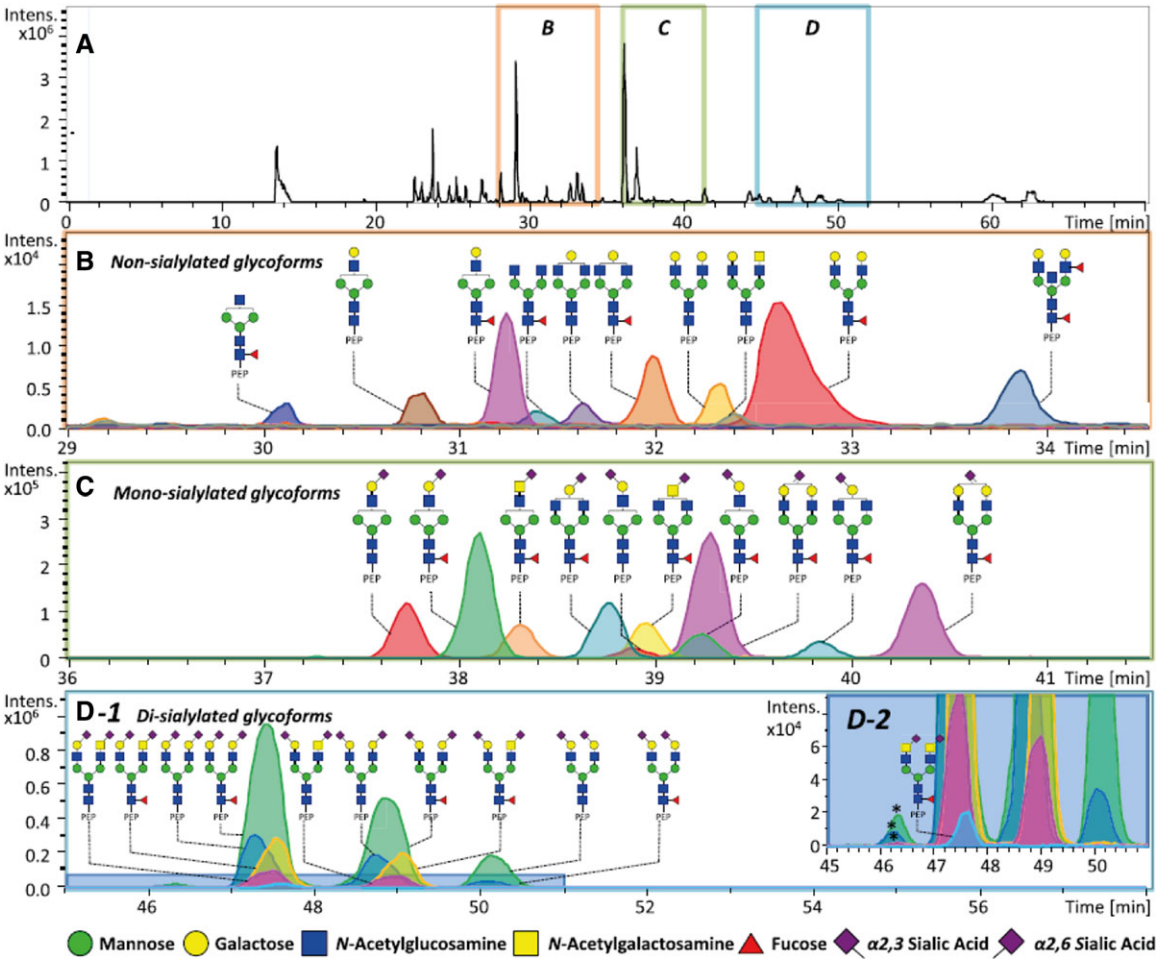


Figure 5. CZE-ESI-MS analysis of PSA tryptic (glyco)peptides. (A) Base peak electropherogram of a tryptic digest with three distinct defined clusters: clusters with only non-sialylated (B), mono-sialylated (C) and di-sialylated (D) glycopeptides of PSA. A total of 75 different glycopeptides were identified. Not assigned peaks are labeled with a '*' in D-2. The 'PEP' label illustrates the tryptic peptide sequence $N_{69}K$ to which the glycan is attached. Reprinted with permission [76]. Copyright © 2018 Springer Nature Limited.

a major improvement compared to individual CZE-ESI-MS (~70% more peptides) and RPLC-ESI-MS (~35% more peptides). Giorgetti et al. used CZE-MS on the glycopeptide level for relative quantification of glycosylation profiles of various mAbs, including the discrimination of Infliximab-Remicade® and its biosimilar [80]. Although being important for many biopharmaceuticals and in the context of clinical diagnostics, *O*-glycosylation is usually less studied than *N*-glycosylation. An acetone-based precipitation method for the enrichment of *O*- and *N*-glycopeptides, derived from various glycoproteins, was developed [81]. *O*-glycopeptides exhibited a different behavior compared to *N*-glycopeptides, potentially allowing more selective enrichment procedures.

Glycosaminoglycans (GAGs), also applied as pharmaceuticals, are unbranched acidic polysaccharides that consist of disaccharide repeating units. The typical approach to analyze these molecules involves the treatment with one or more lyases to generate oligosaccharides (typically disaccharides to decasaccharides) for further analysis by LC or CE. CZE in reverse polarity mode represents a promising method for the separation of sulfated GAG chains, due to their anionic nature. In this regard, Lin et al. developed a CE-MS method (negative ion mode) for the characterization of heparin/heparan sulfate derived disaccharides [82]. In addition, Sanderson et al. evaluated the influence of different coatings (neutral and cationic) and additives (formic acid, diethylamine) to reduce analysis time and improve sample performance, especially for larger oligosaccharides [83]. Utilizing a cationic coating, it was possible to differentiate between stereoisomeric tetrasaccharides, showing the potential of these methods. Future work will be dedicated to expand these setups for CID tandem MS analysis regarding oligosaccharide sequencing. The non-sulfated GAG hyaluronic acid (HA) is a key molecule involved in skin moisture, elasticity and structure. The kinetics of the degradation of HA by hyaluronidases was studied utilizing CE-UV/MS and different synthesized oligosaccharides were evaluated as potential inhibitors/activators in the context of preventing skin aging or diseases [84].

© 2018 WILEY-VCH Verlag GmbH & Co. KGaA, Weinheim

3.4 Biomarkers: peptides, metabolites and nucleic acids

Peptides and polar metabolites exhibit great potential as biomarkers for a variety of diseases. However, since disease states are complicated and biological variability is high between individuals, large-scale studies exploring a large number of compounds combined with powerful multivariate data analysis seems to be most promising in the field. Since CE-MS has proven its suitability for the analysis of hydrophilic compounds such as peptides and metabolites from small injection volumes with high separation efficiency, the number of applications in the context of biomarker identification is increasing.

Biomarker identification is performed in different biological fluids, blood being one of the most promising amongst them. In recent studies, metabolites and especially amino acids were identified as biomarkers in blood for amyotrophic lateral sclerosis [85], chronic kidney disease (CKD) [86], major depressive disorder [87], onchocercias infection [88], osteoporosis [89], Parkinson's disease [90], pancreatic cancer [91], urinary tract symptoms [92] and metabolic syndrome in postmenopausal women [93] by CZE-MS. For identification and accurate quantification of biomarkers for inborn errors of metabolism from dried blood spots, DiBattista et al. developed a multiplexed separation platform [94]. Based on multi-segment injection (MSI)-CE-MS, the method provides comparable sample throughput to flow injection analysis-tandem MS but with increased selectivity. MicroRNAs (miRNA) play an important role in a variety of cellular processes and can be associated with several diseases. Pero-Gascon et al. developed a SPE-CE-MS method for the analysis of miRNAs in serum after offline sample preparation [95]. The potential of this method was demonstrated by detecting specific microRNAs only in patients suffering from B-cell chronic lymphocytic leukemia.

Extensive research is also conducted on the identification of biomarkers from urine, since it is a non-invasive and easily obtainable body fluid. Especially the potential of peptides as biomarkers has been evaluated in recent publications. Schönemeier et al. reported possible peptide biomarkers to distinguish between pancreatic cancer and chronic pancreatitis in urine [96]. Other applications in cancer research include genitourinary [97] and bladder cancer [98]. Belczacka et al. focused on the identification of tumor-specific peptide markers by targeting alterations in the urine peptidome by tumor-related inflammation [99]. They collaborated with patients suffering from different types of cancer. Levels of 193 different peptides were combined to a single multi-dimensional marker. Sensitivity and specificity of this approach were estimated for the detection of tumors of all cancer types as 69 and 81%, respectively. This shows that tumor-specific alterations can be observed in the urine peptidome, independent from the type of cancer. The application of multi-dimensional markers has also resulted in promising results for the diagnosis of other diseases. CKD273 represents a multiple peptide biomarker developed for the diagnosis of CKD, combining levels of 273 peptides using support vector machine algorithm to result in one single classifier [100]. It has been applied multiple times for the diagnosis of CKD and even other diseases since its initial publication. CKD273 was recently used to predict mortality in individuals with type 2 diabetes [101] and their response to albuminuria treatment [102]. Other examples for the application of multi-dimensional marker were published [103, 104], and the application of CE-MS in urinary peptidomics for the diagnosis of CKD was reviewed recently [105]. Urinary peptidomics by CE-MS was furthermore used for the identification of biomarkers for chronic obstructive pulmonary disease [106], diastolic left ventricular dysfunction [107], end-stage renal disease [108], chronic graft-versus-host disease [226], non-alcoholic fatty liver disease [109] and systemic lupus erythematosus [110]. A chiral CE-MS method was published by Švidrnoch to determine D/L-2-hydroxyglutaric acid without derivatization in urine as biomarker for a rare neurometabolic disorder [111].

Saliva represents another non-invasive biological fluid and biomarker discovery was performed for oral [112–114] and pancreatic [91] cancer. Metabolomic profiling of cerebrospinal fluid (CSF) was performed to identify biomarkers for Alzheimer's disease [115]. Prior et al. developed a CE-MS method for the enantioselective separation of fluorenylethylchloroformate- and FMOC-derivatized amino acids from CSF [116, 117]. Fuji et al. analyzed postmortem brain tissue of schizophrenia patients and identified 29 differentially accumulated metabolites compared to the control group [118]. Yamakawa et al. performed metabolic profiling to differentiate tumor types of gastric cancer [119] and Saito et al. profiled low molecular weight compounds in hepatocellular carcinoma [120]. Tu et al. separated and identified peptides from an α_{s1}-casein digest to find possible angiotensin-I-converting enzyme inhibitors [121].

Besides biomarker discovery, there are CE-MS applications for the analysis of non-clinical peptides. One example is the analysis of cyclic peptides that can serve as precursors for peptide nanotubes synthesis [122]. Highly hydrophobic peptides, such as temporin, were successfully analyzed by NACE [123].

3.5 Metabolite analysis and metabolomics

Based on number of publications in the covered timeframe of this review, metabolite analysis constitutes the most extensive research field using CE-MS. As reported above, metabolite analysis is widely applied for the identification of biomarkers, however, related publications cover a considerably broader spectrum of applications. Recent reviews summarized advances in the field, with two publications specifically focusing on metabolomics using CE-MS [124, 125]. The recent boost in publications applying CE-MS for metabolomics may be partly due to the rise of companies such as Human Metabolome Technologies Inc. (HMT), based in Tsuruoka, Japan. HMT offers complete solutions for targeted and

© 2018 WILEY-VCH Verlag GmbH & Co. KGaA, Weinheim

non-targeted metabolomic analysis of various types of biological samples. Standard methodologies, as provided by HMT, offer the potential to improve reliability and inter-study comparison of clinical studies. In fact, when taking all metabolite-related publications of this review into account (including applications for biomarker discovery) roughly one third of the publications were using HMT methodology.

Besides previously mentioned biomarker discovery, metabolite profiling on human biofluids was also used in more general research on metabolism, including the analysis of serum/plasma [126–130], urine [131–135] and saliva [136]. Yamamoto et al. showed a MSI separation of anionic metabolites with over 230 repeated injections of urine samples for the validation of a multiplexed separation platform demonstrating the ability of CE-MS for robust high throughput screening [131]. This high throughput multi-segmented approach was applied for a non-targeted sweat analysis of infant cystic fibrosis patients, associating several ionic metabolites to the disease which could be used as future biomarkers [137]. Harada et al. conducted a large-scale study to assess the reliability of absolute quantification of plasma polar metabolites [128]. They analyzed over 8000 plasma samples, quantifying 94 metabolites. Additionally, over 100 quality control standards were analyzed during the course of the study. Coefficients of variance for the QCs were below 30% for 80 of the 94 metabolites, demonstrating acceptable reproducibility. Quantification results of creatine and uric acid were compared to the results from enzymatic assays performed in independent clinical laboratories and Passing-Bablok regression confirmed good correlation. Overall, the study demonstrated the suitability of CE-MS for large-scale metabolomic studies.

Rodents, rats and mice mainly, are frequently used as model organisms for basic research on metabolism. Metabolic profiling was performed on rodent muscle [139, 234], heart [140, 141], liver [142], brain [143], intestinal [144, 145] and glioma [146] tissue, arterial cells [147] as well as on rodent serum/plasma [144, 145, 148–151], urine [149] and feces [145, 152]. CE-MS was furthermore used for research on the metabolism of microorganism [153–158], plants [138, 159–163] and mushroom [164]. Additional publications are included in Table 5.

EOF fluctuations and suction effects when coupling CE to MS may hamper reproducibility of migration times. To overcome this problem, effective mobilities, a characteristic feature of chemical compounds, can be calculated. Gonzalez-Ruiz et al. developed a novel software to calculate effective mobilities and align feature lists obtained from CE-MS-based metabolic profiling [165]. The conversion of migration times is based on either a known EOF flow or by a substance with known mobility. The application of effective mobilities reduces variation, enhances robustness and feature identification and enables data alignment.

Due to the high variety in physicochemical properties of metabolites, CE-MS is widely used in multiplatform approaches with complementary separation principles to gas and liquid chromatography as shown by the group of Coral Barbas for the analysis of metabolic biomarkers for obesity [126, 166] or cancer [129]. Li and co-workers analyzed tobacco leaves in different stages of development, where CE-MS allowed the determination of 89 out of 412 metabolites (saccharides, phosphates and polyamines) that were not covered by LC and GC [159]. Combinations of RPLC with CE were applied for the analysis of aqueous humor [167] and luminal tissue [145] to cover a broader range of analyte polarities. Ortitz-Villanueva et al. compared two different workflows of an approach based on multivariate curve resolution–alternating least squares (MCR-ALS) for the combination of LC-MS and CE-MS data. They reported that the fusion of the datasets prior to MCR-ALS analysis was more effective in identifying low abundant metabolites [168]. A combination with imaging MALDI-MS for non-targeted metabolomics in different regions of ischemic hearts was able to discover a heterogeneity in carbohydrate metabolism 10 min after initiation [140].

3.6 Pharmaceutical and clinical applications

Biological fluids are also analyzed in the pharmaceutical and clinical context, e.g. for the determination of pharmacologically active substances. Maráková et al. reported a method for fast and reliable drug monitoring in biological fluids for the determination of azathioprine, selected metabolites and co-mediated drugs. [169]. Piestansky et al. reported a comparison of a 2D ITP-CZE-UV method with CZE-MS for the monitoring of the drug varenicline in human urine. [170]. Both methods exhibited comparable performance since MS detection proved to be more sensitive, thus compensating the lack of sample clean-up and preconcentration by the omitted ITP dimension. Another example of drug monitoring in human urine was presented by Hernández-Mesa et al. [171]. They reported a method comparison between MEKC-MS and CZE-MS for the monitoring of eleven 5-nitroimidazoles and their metabolites, applying molecular imprinted solid phase extraction for sample clean-up. CZE-MS offered higher selectivity than MEKC-MS with LODs comparable to those obtained with LC methods. Attimarad et al. presented a method for the determination of vildagliptin in rat plasma including its application to a pharmacokinetic study [172].

The abuse of (prescription) drugs and their availability on the illegal drug market represents a big concern in terms of implications on society and public health. Švidrnoch et al. presented a novel method for the determination of nine designer benzodiazepines in human blood serum after liquid-liquid-extraction by NACE-ESI-MS/MS [173]. NACE is considered to be ideal for coupling with ESI-MS due to the high volatility of the organic solvents. Separation was performed in a semi-permanently coated capillary and LOD's of 1.5 to 15 ng/mL were achieved. Dos Santos et al. investigated amphetamines and derivatives in natural weight loss pills and dietary supplements after QuEChERS extraction by CZE-MS/MS [174]. DiBattista et al. recently introduced a novel method for a broad screening of drugs of abuse and metabolites in human urine by MSI-CE-MS [175]. They demonstrated simul-

© 2018 WILEY-VCH Verlag GmbH & Co. KGaA, Weinheim

taneous determination of more than 52 drugs of abuse by MSI-CZE-MS/MS in one single run after injection of ten samples.

In another study, Maráková et al. demonstrated a CE-MS method for identification and quantification of active drug contents in six commercial pharmaceuticals used for Crohn's disease treatment, which can be applied in a single- or multidrug therapy. [176]. Due to the high sensitivity, demonstrated by low LODs (25–286 ng/mL), the presented method can be useful for drug quality control labs. Schejbal et al. introduced a new method for the screening of ß-secretase inhibitors, a target in Alzheimer's disease treatment [177]. The inhibition study was performed by identification and quantification of the decapeptide SEVNLDAEFR, a known substrate for ß-secretase and its two proteolytic products SEVNL and DAEFR by CZE-MS with LOD and LOQ of 5 and 15 nM, respectively.

Separation in CE-MS can be fast when using short capillaries. Using 25 cm capillaries could increase the speed to about 1 min, when using a strong EOF and co-migrating ions as demonstrated for the analysis of enantiomeric amphetamines and related compounds using (18-crown-6)tetracarboxylic acid as chiral selector [178].

Metallodrug complexes play a major role as pharmaceuticals, especially for cancer treatment. In this context, CE-ICP-MS has proved its worth as analytical technique for the characterization of the biodistribution of these drugs, including their binding properties to various biomolecules [179–183]. For example, Holtkamp et al. characterized metabolites of RAPTA-C and cisplatin in cell culture medium [179]. Interestingly, the amounts of observed protein adducts were affected by the type of cell culture medium. Artner et al. presented investigations on the activation mechanism and binding preferences of metal-based anticancer agents by CZE-MS [180, 181]. They highlighted the binding specificity of, mainly ruthenium-based, anticancer agents on a molecular level with single-nucleotide resolution.

Tascon et al. developed a CE-MS method for the identification of ppt-levels of harmala alkaloids in algae [184]. By combining CE-MS with online SPE, 1000-fold preconcentration was achieved compared to CE-MS. Liu et al. analyzed active ingredients from *Radix tinosporae* and characterized several compounds potentially being responsible for its anti-inflammatory or anti-viral effects [185]. NACE-MS based on ammonium acetate in ACN-methanol mixtures was used to separate a total of 6 relevant compounds.

3.7 Food and environmental analysis

Due to its selectivity and potential tolerance to non-ionic matrix components, CE-MS has been applied often in the field of food analysis. Analytes of interest include mainly amino acids, amines, carboxylic acids and carbohydrates. To obtain the necessary sensitivity, the injection of large volumes is aspired, requiring a low conductivity matrix. Such a sample can be obtained by precipitation of salts or by ion exchange chromatography. Daniel et al. removed the excess of sulfate, present in the sample after hydrolysis of carbohydrates by sulfuric acid, by the addition of barium ions, increasing sensitivity for monosaccharides in the subsequent CE-MS measurement [186]. Kerrin et al. applied cation exchange clean-up prior to injection for the analysis of the neurotoxic amino acid β-*N*-methylamino-L-alanine in seafood, achieving sub-ppb sensitivity using a triple quadrupole (TQ) MS [187]. Sensitivity in the low μg/kg-range was achieved for the determination of tetracyclines and quinolones in milk after SPE sample preparation [188]. Benzimidazoles were determined in meat at low μg/kg-level after dispersive liquid-liquid extraction [189]. CE-MS has also been applied for the analysis of fatty acids [190]. Although anionic separation was performed, sensitivity could be increased especially for short and medium chain lengths by the addition of a cationic ion pairing reagent and ESI in positive ion mode. Ruzik and Kwiatkowski used a combination of CE-ICP-MS and CE-ESI-TQ-MS for the characterization of zinc binding ligand species in goji berries extract [191]. In this way, it could be shown that zinc can be complexed by different groups of compounds, including amino acids, carotenoids, phenolic acids, flavonols and stilbenoids. Saxitoxin, a paralytic shellfish toxin, can potentially harm human health through the food chain. For this reason, He et al. developed an indirect method for saxitoxin quantification using CE-ICP-MS and Eu^{3+} chelate labeling [192].

Environmental applicability of CE-MS is hampered by its weak concentration sensitivity. In this context, sample preparation as well as online preconcentration techniques play a crucial role. Malá and Gebauer developed, characterized and applied a capillary isotachophoresis (CITP)-MS method for the analysis of two hydroxyl-triazines in water [193]. Due to the large injection volumes in CITP (100 μm x 100 cm capillaries), LODs down to 100 ng/L can be achieved using single ion monitoring in a quadrupole MS without any offline preconcentration. Extension of the ITP principle to an additional pH-gradient allows the focusing of weak acids such as sulfonamides in a so-called inverse 'electromigration dispersion' coupled to mass spectrometry using a maleic acid/2,6-lutidine system as leading and terminating electrolyte [194]. The wide application of fluoroquinolones (FQ), a class of synthetic antibiotics in the pharmaceutical and veterinary context, is one cause of contamination in environmental water. Zhang et al. presented a method for the determination of eight FQs in lake water by CZE-MS with preliminary offline immunoaffinity extraction (IAE) for sample enrichment [195]. The use of a polyclonal antibody for IAE enabled the simultaneous detection of all eight FQs with LODs from 1.2 to 5.0 nM.

Amino acids and amines were used to characterize soil in the context of its hydration/dehydration properties [196–198]. The characterization of naphthenic acids in overburden of oil sands with respect to its impact on environmental waters was performed by CE-MS after conversion to naphthenic amines [199, 200].

© 2018 WILEY-VCH Verlag GmbH & Co. KGaA, Weinheim

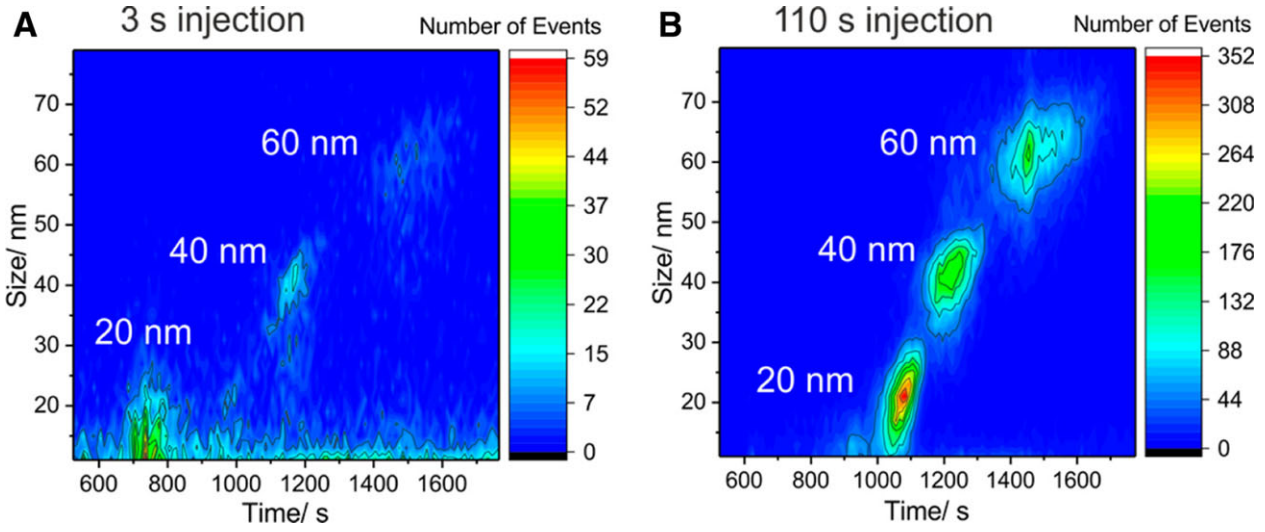


Figure 6. Two-dimensional color maps of CZE-SP-ICP-MS analysis of silver NPs ($^{107}Ag^{+}$) with different particles sizes (20–60 nm): 3 s injection time without REPSM (A) and 110 s injection time with REPSM (B). Different particle sizes are fully resolved for both injection modes. Background observed in (A) is still present in (B) but not apparent due to the scaling. Increase in particle detection by REPSM: 14.3 ± 1.5 for 20 nm, 21.0 ± 4.2 for 40 nm and 27.7 ± 4.9 for 60 nm particle size. Reprinted with permission from [207]. Copyright © 2018 American Chemical Society.

Thermodynamics of actinides are essential in the context of long-term safety assessment of repositories for nuclear waste disposal. CE-ICP-MS is commonly applied for radioactive metal analysis. In this regard, Tasi et al. investigated the redox behavior and solubility of plutonium under alkaline and reducing conditions using ICP-sector-field-MS detection [201]. Natural organic matter (NOM) can play a major role in the mobilization and immobilization of radioactive metal ions due to their complexation and colloid formation tendency. For this reason, the complexation of U(VI) and Eu(III), as chemical homologues of trivalent actinides such as americium, by NOM was investigated by the Kautenberger group [202, 203]. Furthermore, the long-term exposure of actinides to the human body is of major interest. CE-ICP-MS has been used for investigation of actinide-protein binding properties [204, 205].

3.8 Nanoparticles

Nanoparticles (NPs) play an important role in many fields of science, including medicine, physics, optics, electronics and consumer products in general. Since many different properties are responsible for the characteristics of NPs, multimethod approaches are commonly used. Exemplarily, NP number concentration and size distribution are relevant parameters directly affecting the interaction of NPs with biological systems. In this context, CE hyphenated to ICP-MS represents a promising technique for NP characterization.

The Engelhard group utilized CZE methods hyphenated with single-particle (SP)-ICP-MS for the characterization of gold and silver NPs [206–208]. Characteristics of SP-ICP-MS include individual injection of particles combined with short dwell times, which enables the rapid measurement of NP size, size distribution and particle number concentration. The BGEs of these methods comprised SDS as additive, which, among other things, prevents coalescence of NPs and thus improves the overall separation performance. For the characterization of silver nanoparticles with different sizes (20, 40, 60 nm) they incorporated a prototype data acquisition with remarkable high time resolution (5 μs, 100% duty cycle) [207]. In addition, reversed electrode polarity stacking mode (REPSM) was applied as preconcentration step, allowing injection times up to 110 s, to further increase sensitivity, as shown in Fig. 6. Subsequently, this system was utilized to characterize silver NPs with similar sizes but different surface coatings, which represents an important property in the context of understanding the toxicity of various types of NPs [208]. In addition to various surface coatings, Qu et al. investigated the influence of different matrices on silver NPs, including Suwane River humic acid solution and fetal bovine serum using CZE-ICP-MS [209]. Matczuk and co-workers characterized the protein corona of gold NPs at equilibrium conditions by exposing the NPs to bovine and human serum [210]. This study was later expanded to different particle geometries (rod- and spherical-shaped), size, surface functionalization, applied dose (NP-to-protein molar ratio) and exposition time [211, 212]. Subsequently, they investigated the cellular uptake of gold NPs in artificial cytosol (normal and cancer conditions) [213]. Here, the application of MS/MS is proposed for future studies, in order to be able to identify Au species in real cancer cytosol.

© 2018 WILEY-VCH Verlag GmbH & Co. KGaA, Weinheim

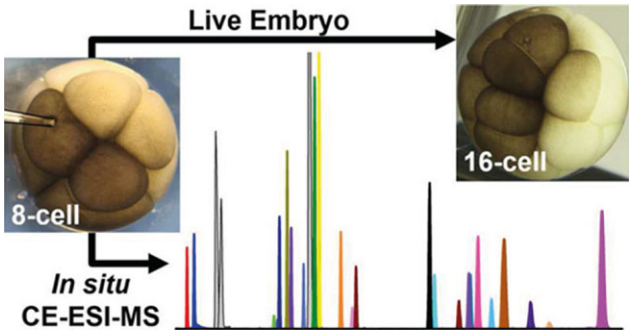


Figure 7. Microprobing to extract cellular content from single embryotic cells for subsequent CZE-MS metabolic profiling. Collection of 10–15 nL was possible, representing ~10% of the overall cellular content. Surprisingly, cells were able to further divide after analysis, demonstrating the possibility to analyze live cells. Reprinted with permission from [219]. Copyright © 2018 American Chemical Society.

3.9 Single-cell analysis

In conventional biochemical assays, cell properties are averaged over a whole population of cells. Although research conducted with such techniques resulted in an increasing understanding of cellular processes, crucial information gets lost by averaging. Transitional states of cells and cell-cell communication as well as cell-cell heterogeneity can solely be elucidated by single-cell analysis. Among the most applied techniques for single-cell analysis are flow cytometry, fluorescence microscopy and single cell RNA-sequencing, the latter only possible in combination with PCR-amplification. However, to examine single cells on a proteomic or metabolomic level, novel methodologies are needed. New developments in single-cell analysis were recently reviewed [214, 215] with one review specifically focusing on mass spectrometry methods [216]. Mass spectrometry is a suitable technique for the analysis of single cells and molecular identification of cellular compounds, if sufficient sensitivity is provided. Coupling of mass spectrometry with small-scale separations such as nanoLC and CE are promising for extensive proteomic and metabolomic profiling of single cells.

Nemes' group intensively worked on the characterization of single cells from *Xenopus* embryos to elucidate how body symmetry breaks during early embryonic development. CE-MS was successfully applied to the metabolomic profiling of single blastomeres 'manually' dissected from an 8-cell embryo. By direct comparison of metabolic profiles, they found 10 metabolites accumulated significantly different in left and right cells in the embryo [217]. In a subsequent study, the same group applied CE-MS for the proteomic profiling of single embryonic cells of *Xenopus* [218]. Cell lysis was performed, and proteins were precipitated and subsequently digested with trypsin. In total, 130–150 different protein groups were identified by CZE-MS. The methodology was further optimized by developing a microsampling strategy to aspirate a small portion of the cellular content [219]. For this method, a 20 μm id capillary was mounted on a motorized xyz stage and could be precisely remote controlled, which enabled the collection of 10–15 nL cellular content. The novel method was compared to the whole-cell dissection method applied in previous studies. Microprobing increased sampling speed, reduced damage to the probed and surrounding cells and enabled multiple probing of the same cell. Surprisingly, the authors observed that even after probing, cell division continued, proving the applicability of the method to analyze live cells (Fig. 7). CE-MS metabolomic characterization of the single cells was enhanced by microsampling, as can be seen by an increased number of theoretical plates and consistent feature detection although the injected sample amount was 10–20 times smaller compared to whole-cell dissection.

In another publication, the group developed a CE-MS method, including RP pre-fractioning on a ZipTip column, to identify proteins from small volumes of mammalian neuron digests [22]. The inclusion of a three-step RP fractioning improved overall separation efficiency, sensitivity and number of peptide identifications compared to direct CE-MS analysis. Downscaling of the method to the injection of ~500 pg protein digest, representing the protein amount of a single neuron, resulted in the identification of 141 proteins per analysis. Although this demonstrated the applicability of the method for the analysis of sub-nanogram protein amounts, it is worth mentioning that the RP fractioning was performed with ~1 μg tryptic digest, representing ~2000 neurons. Thus, further optimizations of the overall workflow are needed to apply the method for the direct measurements of single neurons.

As previously mentioned, Comi et al. combined the advantages of MALDI-MS and CE-ESI-MS in a combined method for the analysis of single pancreatic islet cells [29]. Cell types were rapidly identified by MALDI-MS according to their peptide profile. Analyte extraction was subsequently performed from identified target cells on the MALDI-plate by a novel liquid microjunction interface for CE-MS analysis.

© 2018 WILEY-VCH Verlag GmbH & Co. KGaA, Weinheim

This offline hyphenation enables combined detection of lipids, peptides and small ionic metabolites including amino acids in single cells.

4 Concluding remarks

CE-MS has proven its applicability in various analytical fields. While instrumental developments, especially regarding improved interfacing between CE and MS continues, commercially available interfacing solutions have demonstrated their suitability for routine applications. Especially in terms of biomarker discovery and metabolism studies, CE-MS is developing toward a standard analytical technique besides GC- and LC-MS, as can be seen by the vast number of publications in the field of proteomics and metabolomics. Large-scale studies recently demonstrated reliability, reproducibility and long-term stability of CE-MS methodologies. Advancements were also made toward high-throughput methods by application of MSI and fast separations in different fields. The possibility to reduce dead times by MSI is unique for electrophoretic systems since no gradient is applied. Future research on this matter will probably further boost throughput on electrophoretic platforms.

The complementarity between chromatographic and electrophoretic methods has been demonstrated frequently. New developments are heading toward exploiting this characteristic by combining the two systems. Offline coupling, including fraction-collection by RPLC and subsequent CZE-MS analysis was shown in recent bottom-up proteomic studies. Due to a high degree of orthogonality, this may result in a substantial increase in peak capacity. RPLC and CZE were also combined by integrative approaches. Here RPLC-MS and CZE-MS are performed independently, and results are combined. This has proven to be especially helpful in the field of metabolomics due to the high variety of physicochemical properties of metabolites. In future, combination of different analytical systems may play a crucial role to overcome the problem of increasing sample complexity and needs of multiple analyte characterization.

CE inherently uses small injection volumes. This often hampers concentration sensitivity, thus, the development of preconcentration and stacking techniques is ongoing to overcome this problem. However, in the field of single-cell analysis, handling of extremely small sample amounts is mandatory, making CE a perfect technique for applications in this field. In combination with mass spectrometry, characterization of analytes from small sample amounts and even single cells is possible. When combined with suitable sample taking devices, CE-MS offers great potential in single cell analysis, as shown by the possibility to analyze live cells.

In conclusion, research conducted during the last two years indicates that CE-MS will further develop toward getting a routine system in biochemical analysis. Throughput and automatization will be further optimized and methodologies combining chromatographic and electrophoretic separation systems hold the potential to handle analytes with different physicochemical properties. Research on single-cell analysis is still at an early stage, but CE-MS has been proven its high potential for single-cell characterization.

5 Tabulated summary of CE-MS applications

This section summarizes the applications of CE-MS mentioned in the main text and additional publications. The tables are structured according to the field of application and contain methodological parameters as well as a comment column with either results or remarks of the respective publication. Abbreviations used in the tables are listed below the table if they have not been previously introduced in the main text. This section contains the following tables:

Table 1: Protein analysis and proteomics (intact and digested proteins, this does not include monoclonal antibodies)
Table 2: Monoclonal antibodies
Table 3: Glycans and saccharides (also includes glycopeptides)
Table 4: Peptides and biomarkers (includes clinical studies with peptides, metabolites and other compounds as possible biomarkers)
Table 5: Metabolite analysis and metabolomics (includes papers on research on metabolism, nutrition and disease on microorganisms, cell cultures, plants and mammals as well as humans)
Table 6: Pharmaceutical and clinical applications (publications on identification of active substances in drug formulations and biological fluids as well as basic pharmaceutical research)
Table 7: Environmental and food analysis (CE-MS methods for the analysis of environmental and food samples)
Table 8: Nanoparticles
Table 9: Single cell analysis

The authors thank Hoffman-La Roche Ltd. (Basel, Switzerland) for financial support. The authors also want to thank an unknown reviewer for the detailed and very helpful remarks.

The authors have declared no conflict of interest.

© 2018 WILEY-VCH Verlag GmbH & Co. KGaA, Weinheim

Table 1. Protein analysis and proteomics (intact and digested proteins, this does not include monoclonal antibodies)

Analytes/samples	Mode	Coating	BGE	Interface; sheath liquid	MS	Comments	Ref.
β_2-microglobulin (two conformers)	CZE(N)	FS	50 mM ammonium hydrogencarbonate	(1) SFI, 1% FAc in 50% IPA (2) Sheathless (CESI 8000)	TOF	Sheathless interface enables conformer identification by charge-state distribution	[44]
AT conformers and dimers	CZE(N)	PVA	50 mM ammonium acetate	SFI; 50% IPA + 14 mM ammonium acetate	TOF	Separation of AT conformers. Identification of conformers by their charge state distributions	[45]
Analysis of protein complexes	CZE(N)	FS/PAM	25 mM ammonium acetate	Sheathless (CESI 8000)	OT	Native separation and characterization of model proteins, mAb, *E. coli* ribosomal isolate	[46]
Human tissue transglutaminase TG2	CZE(N)	FS	15 mM tris-acetate	SFI, 50% MeOH + 0.5% HAc	IM-TOF	Simultaneous measurement of conformational changes and enzymes activity	[47]
Fibroblast Growth Factor 21 fused to a human Fc fragment	CZE(N)	LPA	30% HAc	SFI; sheath liquid n.p.	TOF	Determination of ADME parameters in vivo	[48]
Glycosylated tuberculosis antigens	CZE(N)	PB-DS-PB	1.5 M HAc	SFI; 50% IPA + 0.1% FAc	TOF	Separation of chemically glycosylated proteins	[49]
E. coli cell lysate	CZE(N)	LPA	5-10% HAc/ 0.1-0.5% FAc	SFI; 10% MeOH + 0.5% FAc	OT	Identification of 600 proteoforms	[50]
Model proteins/ model mAb	CZE(N/R)	Different coatings	1 M HAc	50% IPA + 0.2% FAc	TOF	Successful removal of excess SDS by an in-capillary approach	[51]
Myoglobin, cytochrome C	CIEF	LPA	0.4% Pharmalyte® (3-10) A: 0.1% FAc C: NH_3 plug (0.3%)	SFI, 10% MeOH + 0.1% FAc	OT	Successful CIEF-MS method with a short plug of NH_3 for focusing	[52]
Mixture of model proteins	CIEF	PVA	Varying ampholytes conc. A: 50 mM FAc C: 100 mM ammonium hydroxide	SFI, 80% MeOH + 0.2% FAc	TOF	Sequential injection of carrier ampholytes and sample is efficient for protein characterization	[53]
Antibody mAb1 digest	CZE(N)	LPA	20% HAc, 15% DMA	Sheathless (CESI 8000)	LIT	Improved resolution and S/N for proteolytic peptides of the antibody	[54]
Antibody-drug conjugate digest	CZE(N)	LPA	20% HAc, 15% DMA, 1% m-nitrobenzyl alcohol	Sheathless (CESI 8000)	OT	100% sequence coverage	[55]
Bovine lactoferrin, tryptic digest	CZE(N)	FS	10% HAc	Sheathless (CESI 8000)	TOF	CE-MS beneficial for peptides with larger size-to-charge ratios compared to UHPLC-MS	[56]
Tryptic digested vitreous humour sample	CZE(N)	FS	20% ACN + 0.94% FAc	N.p.	TOF	Identification of 5 potential protein biomarkers for RVO	[57]
Yeast tryptic digest	MSI-CZE(N)	LPA	5% HAc	SFI; 10% MeOH + 0.5% FAc	OT	MSI can double the peptide identification rate	[58]
Human lymphoblastic T-cells digest	CZE(N)	DMA-GMA-MAPS	N.p.	Sheathless (CESI 8000)	OT	Identification of 62 000 peptides of 6100 proteins	[59]

(*Continued*)

© 2018 WILEY-VCH Verlag GmbH & Co. KGaA, Weinheim

Table 1. Continued

Analytes/samples	Mode	Coating	BGE	Interface; sheath liquid	MS	Comments	Ref.
Xenopus laevis eggs protein digest, BSA digest, *E. coli* digest	CZE(N)	LPA	1 M HAc	SFI; 10% MeOH + 0.5% FAc	OT	Application of inline SPE. of 365 peptides of an *E. coli* digest	[60]
Mixture of digested standard proteins; mouse brain/liver digest	CZE(N)	LPA	5% HAc	SFI; 10% MeOH + 0.2% FAc	TOF	CZE-MS method with high injection volume and 140 min separation window	[61]
Myelin basic protein purified from mouse brain tissue	CZE(N)	Neutral	0.1 M HAc	Sheathless (CESI 8000)	OT	Multiple PTM identification in MBP	[62]
Protein standard mixture, tryptic digest	CZE(N)	FS/N	0.1 M HAc/ 0.1% FAc	Sheathless (CESI 8000)	OT	Separation of native and deamidated (Asp/iso-Asp) peptides	[63]
Stressed TRI-1144 (4.5 kDa peptide)	CZE(N)	PB-DS	Ammonium formate/ ACN/IPA (60/35/5)	SFI; 50% IPA + 0.1% FAc	TOF	Characterization of deamidated and deacetylated peptide species	[64]
Synthetically modified peptides	CZE(N)	FS	10% HAc	Sheathless (porous tip)	OT	Complementary phosphopeptide identification by CZE-MS and nanoLC-MS	[65]
Bet v a1 from birch pollen	CZE(N)	FS	10 mM ammonium hydrogencarbonate	SFI; 75% MeOH + 0.1% FAc	OT	Identification of nitration sites by combined top-down and bottom-up approach	[67]
Xenopus laevis fertilized egg digest	CZE(N)	LPA	5% HAc	SFI; 10% MeOH + 0.5% FAc	OT	4100 protein and 22,535 peptide identifications by RPLC-CZE-MS/MS	[68]
Mouse brain homogenate tryptic digest	CZE(N)	LPA	5% HAc	SFI; 10% MeOH + 0.2% FAc	OT	Identification of 8200 protein groups and 65,000 unique peptides by SCX-RPLC-CZE-MS	[69]
E. coli cell lysate	CZE(N)	FS	10% HAc	Nano-SFI; 50% MeOH + 10 mM ammonium acetate	OT	Identification of 850 proteins and 5700 proteoforms from *E. coli* by SEC-RPLC-CZE-MS/MS	[70]

ADME: absorption, distribution, metabolism, and excretion, **AT**: antithrombin, **C/A**: catholyte/anolyte, **conc.**: concentration, **DS**: dextran sulfate, **FAc**: formic acid, **FS**: fused silica, **GMA**: glycidyl methacrylate **HAc**: acetic acid, **HfrEF**: heart failure with reduced ejection fraction, **IPA**: isopropanol, **LIT**: linear ion trap, **LPA**: linear polyacrylamide, **MAPS**: 3-(trimethoxysilyl) propyl methacrylate, **MeOH**: methanol, **N**: normal polarity, **n.p.**: not provided, **OT**: Orbitrap, **PAM**: polyacrylamide, **PB**: polybrene, **R**: reversed polarity, **RVO**: retinal vein occlusion, **SFI**: sheath flow interface

© 2018 WILEY-VCH Verlag GmbH & Co. KGaA, Weinheim

Table 2. Monoclonal antibodies

Analytes/samples	Mode	Coating	BGE/anolyte/catholyte	Interface; sheath liquid	MS	Performance/ Result	Ref.
HCP	CZE(N)	LPA	1 M HAc	Nano SFI; 10% MeOH + 0.5% FAc	OT	Determination of HCP (tryptic peptides) after mAb depletion or non-depletion	[72]
Cetuximab Fc/2	CZE(N)	HPC	I: 200 mM EACA-ammonium acetateO: 25 mM ammonium acetate	Offline coupling to MALDI	MALDI-TOF	Proof of principle for middle-down characterization of Fc/2 charge variants	[28]
Trastuzumab	CZE(1D)-	FS	380 mM EACA, 1.9 mM TETA, 0.05% HPMC	SFI; 50% IPA + 0.2% FAc or 1% HAc	TOF	Online 2D CZE-CZE-MS with mechanical valve, characterization of trastuzumab charge variants including deamidation products	[42]
	CZE(2D)	PVA	0.2/1 M FAc or 0.5/1/2/3/5 M HAc				
Model antibody (mAb X)	CIEF(1D)-	PVA	Servalyt® (pH 3-10/ 6-8) (concentration n.p.) C: 335 mM L-Arg; A: 0.2 M phosphoric acid	SFI; 50% IPA + 1% HAc	TOF	Online 2D CIEF-CZE-MS with mechanical valve, multi heart-cut characterization of mAb X charge variants	[40]
	CZE(2D)	PVA	0.2 M FAc				
Trastuzumab	iCIEF(1D)-	LPA	2% AESlyte® (pH 4-8) C: 0.1% MC + 100 mM NaOH; A: 0.1% MC + 80 mM phosphoric acid	SFI; 50% MeOH + 1% HAc or 50% IPA + 0.5% FAc	TOF	Online 2D iCIEF-CZE-MS with mechanical valve, characterization of trastuzumab charge variants	[41]
	CZE(2D)	PVA	1 M HAc				
Infliximab, Trastuzumab, Bevacizumab, Cetuximab	CIEF	Neutral	1.5% Pharmalyte® (pH 3-10); C: 0.2 M ammonium hydroxide + 15% glycerol; A: 1% FAc + 15% glycerol	Nano-SFI; 20% HAc in 25% ACN or 50% MeOH + 0.5% FAc	TOF	Separation and characterization of mAbs charge variants, correlating with iCIEF-UV	[73]

C/A: catholyte/anolyte, **FAc**: formic acid, **HAc**: acetic acid, **HPC**: hydroxypropyl cellulose, **HPMC**: hydroxypropyl methylcellulose, **I/O**: inlet/outlet, **IPA**: isopropanol, **LPA**: linear polyacrylamide, **MC**: methylcellulose, **MeOH**: methanol, **n.p.**: not provided, **OT**: Orbitrap, **SFI**: sheath flow interface, **TETA**: triethylenetetramine

© 2018 WILEY-VCH Verlag GmbH & Co. KGaA, Weinheim

Table 3. Glycans and saccharides (also includes glycopeptides)

Analytes/samples	Mode[a)]	Coating	BGE	Interface; sheath liquid	MS	Comments	Ref.
N-glycan standards	R	PVA	30 mM ammonium acetate	SFI; 50% IPA + 0.2% ammonium hydroxide	TOF	Twoplex relative quantification of isotopically labeled glycans; 2-AA label ($^{12}C_6$- and $^{13}C_6$) applied.	[74]
N-glycans: protein standards, human serum	N	FS	10% IPA, 0.1% FAc,	Sheathless (CESI 8000)	OT	77 potential glycan structures found in human serum; Methylamidation and APTS label applied	[75]
Monosaccharides, *N*-glycans, *N*-glycopeptides: protein standards	N	N.p.	50% MeOH, 2% FAc	ZipChip (908 Devices); 50% MeOH, 2% FAc	OT	Analysis of monosaccharide, glycan and glycopeptides; Aminoxy TMT label applied	[220]
N-glycopeptides: antibodies, PSA	N	FS	10% HAc	Sheathless (CESI 8000)	TOF	Separation of glycopeptides only differentiating in their sialic acid linkages	[76]
N-glycopeptides: antibodies, PSA, Hp	N	FS	10% HAc	Sheathless (CESI 8000)	TOF	Dopant (ACN) enriched nitrogen gas applied to increase sensitivity for glycopeptide analysis	[13]
N-glycopeptides: PSA in clinical urine samples	N	FS	10% HAc	Sheathless (CESI 8000)	TOF	Development of a PSA assay for urine samples; applicability as diagnostic tool for prostate cancer focus of future studies	[77]
N-glycopeptides: antibodies, Hp	N	FS	0.5% FAc	Nano-SFI; 10% MeOH + 0.1% FAc	OT	Improved resolution and higher sensitivity (same injected amount) compared to nanoRPLC	[78]
N-glycopeptides: hAGP	N	FS	5% FAc	Nano-SFI; 10% MeOH + 0.1% FAc	OT	Offline 2D UHPLC-CZE-ESI-MS; 268 site-specific *N*-glycopeptides (8 sites) for two AGP isomers	[79]
N-glycans, *N*-glycopeptides: mAbs	N	FS	10% HAc	Sheathless (CESI 8000)	TOF	Relative quantification of glycan species; Discrimination of biosimilar; 2-AB label applied (released glycans)	[80]
O- and *N*-glycopeptides: protein standards	N	FS	50 mM HAc, 50 mM FAc	SFI; 50% IPA + 0.05% FAc	TOF	Investigation of conditions for acetone enrichment of *O*- and *N*-glycopeptides using multivariate statistics	[81]
Glycosaminoglycans: heparin/heparan sulfate standards, Arixtra®	R	FS	80% MeOH, 10 mM ammonium acetate	Nano-SFI; 80% MeOH, 10 mM NH_4Ac	OT	Characterization of heparin/heparan sulfate derived oligosaccharides; bottom-up and top-down analysis	[82]
Glycosaminoglycans: heparin/heparan sulfate standards, Enoxaparin®	R	FS DMDCS AHS	70% MeOH, 25 mM NH_4Ac	Nano-SFI; 70% MeOH, 25 mM NH_4Ac	OT	Neutral (DMDCS) and cationic (AHS) coatings improved separation time and peak width	[83]
Glycosaminoglycans: hyaluronic acid standards	R	FS	10 mM NH_4Ac	SFI; 80% MeOH + 0.02% FAc	TOF	Determination of kinetic constants for enzymatic degradation of hyaluronic acid; Di- to Decasaccharides characterized	[84]

a) **Mode: all CZE.**

2-AB: 2-aminobenzamide, **AA**: aminobenzoic acid, **AHS**: aminomethyltriethoxysilane, **DMDCS**: dichlorodimethlysilane, **FAc**: formic acid, **FS**: fused silica, **HAc**: acetic acid, **hAGP**: human α-1-acid-glycoprotein, **Hp**: haptoglobin, **IPA**: isopropanol, **MeOH**: methanol, **N/R**: normal/reversed polarity, **n.p.**: not provided, **OT**: Orbitrap, **SFI**: sheath flow interface, **TEA**: trimethylamine, **TMT**: tandem mass tag

© 2018 WILEY-VCH Verlag GmbH & Co. KGaA, Weinheim

© 2018 WILEY-VCH Verlag GmbH & Co. KGaA, Weinheim

Table 4. Peptides and biomarkers (includes clinical studies with peptides, metabolites and other compounds as possible biomarkers)

Analytes/samples	Mode	Coating	BGE	Interface; sheath liquid	MS	Comments
Human cancer cells [119] Saliva [113, 114] Serum [89, 221]	CZE(N)	FS	1 M FAc	SFI; 50% MeOH + hexakis/reserpine	TOF	Untargeted biomarker discovery (metabolites). Identification of 110 [119], 189 [221] and 83 [115] metabolites
CSF [115]	CZE(R)	Cationic coating	50 mM ammonium acetate	SFI; 50% MeOH + 5 mM ammonium acetate + hexakis/reserpine		
Urine [104, 107, 222] Plasma [222] Cephalic fluid [223]	CZE(N)	FS	0.94% FAc in 20% ACN	SFI [222, 223] / Nano SFI [223] 30% IPA + 0.5% FAc [222] 30% IPA + 0.4% FAc [223]	TOF [104, 222, 223] OT [223]	Untargeted peptidomics
Human urine [96, 98, 101, 102, 108, 109] Mouse urine [224]	CZE(N)	FS	0.25 M FAc in 20% ACN	SFI 30% IPA + 0.5% FAc [96, 98, 101, 102, 224] 30% IPA + 0.4% FAc [109]	TOF	Untargeted urinary peptidomics
Saliva [112] Serum/plasma [88, 90, 92] Human brain tissue [118]	CZE(N)	FS	HMT BGE, pos. mode	SFI 50% MeOH + 0.5 mM reserpine [90] 50% MeOH + 5 mM ammonium acetate [92] N.p. [88, 112, 118]	TOF	Untargeted biomarker discovery (metabolites). Identification of 499 [112], 286 [88], 60 [92] and 300 [118] metabolites. Analysis performed by HMT
	CZE(R)	FS	HMT BGE, neg. mode	SFI; 50% MeOH + 5 mM ammonium acetate + 1 mM reserpine [90] N.p. [88, 92, 112, 118]		
Rat urine [225] Human urine [226]	CZE(N)	FS	1% FAc 20% ACN	SFI; 30% IPA + 0.4% FAc	TOF	Detection of 123 differentially expressed peptides in relation to control
DBS samples of newborns [94]	CZE(N) CZE(R)	FS FS	1 M FAc in 15% ACN 50 mM ammonium hydrogencarbonate	SFI; 60% MeOH + 0.1% FAc 50% MeOH	TOF	MSI-CE-MS for polar metabolites from DBS extracts
Choline, betaine, dimethylglycine in plasma of CKD patients [86]	CZE(N)	FS	5% FAc/ 10% MeOH	SFI; 50% MeOH + 5 mM ammonium acetate	TQ	Identification of possible biomarkers for CKD
Urinary peptides of COPD patients [106]	N.p.	N.p.	N.p.	N.p.	TOF	Urinary peptide content differs between phenotypes of COPD
Urine samples of healthy and CKD patients [103]	CZE(N)	N.p.	N.p.	N.p.	TOF	Identification of seven peptides possibly related to fibrosis
Urine peptide biomarkers of patients with SLE [110]	CZE(N)	FS	N.p.	N.p.	TOF	Development of urine assay for SLE diagnosis
FLEC-derivatized D/L-amino acids in CSF [117]	Chiral CE	FS	150 mM APFO	SFI; 90% IPA + 0.1% FAc	IT	Detection of endogenous levels of D-amino acids in CSF

(*Continued*)

Table 4. Continued

Analytes/samples	Mode	Coating	BGE	Interface; sheath liquid	MS	Comments
FMOC- derivatized amino acids & spiked CSF [116]	Chiral CE	FS	10 mM β-CD in 15% IPA + 50 mM ammonium acetate	SFI; 50% IPA + 10 mM ammonium hydrogencarbonate	IT	LOD of method not sufficient for detection of endogenous levels of D-amino acids in CSF
Separation of D/L-2-hydroxyglutaric acid in urine [111]	Chiral CE	PAM	50 mM ammonium acetate + 25 mM Vancomycin chloride (CS)	SFI; 50% MeOH + 0.5% ammonium hydroxide	TQ	Separation of 2-hydroxyglutaric acid enantiomers without derivatization
Peptide analysis of tryptic casein hydrolysate [121]	CZE(N)	FS	10% HAc/ 100 mM ammonium acetate	SFI; 10% HAc/ 100 mM ammonium acetate	TOF	Novel ACEI peptide identified
Hercynine in urine, whole blood, plasma, and saliva [227]	CZE(N)	FS	5 mM ammonium acetate	SFI; 50% MeOH + 2.5 mM ammonium acetate	Q	Targeted analysis of hercynine
Human liver tissue [120]	CZE(N)	FS	200 mM ammonium acetate	SFI; 50% MeOH + 0.5 mM ammonium acetate	TQ	Targeted analysis
Human plasma of postmenopausal women [93]	CZE(N) CZE(R)	N.p. Cationic coating	N.p. 50 mM ammonium acetate	N.p. SFI; 50% MeOH + 5 mM ammonium acetate + 0.1 μM hexakis	TOF	Targeted metabolite analysis
Human plasma [85]	CZE(N)	FS	5 M HAc	SFI; 50% MeOH + 5 mM ammonium acetate	TQ	Targeted analysis of glutamic acid and cysteine and their metabolites
Circulating μRNAs in serum of cancer patients [95]	CZE(N)	FS	25 mM ammonium acetate	SFI; 80% IPA + 2 mM ammonium acetate	TOF	SPE-CE-MS, LODs ~10 nM
Human urine [97]	CZE(N)	Cationic coating	2% FAc in 50% MeOH	SFI; 50% MeOH + 2% FAc	TQ, TOF	Targeted and untargeted analysis of cationic metabolites
Human urine [99]	CZE(N)	FS	0.25 M FAc in 20% IPA	SFI; 30% IPA + 0.5% FAc	TOF	Urinary peptidomics and identification of 193 peptides
Metabolic profiling of MDD and control patients [87]	CZE(N) CZE(R)	N.p. COSMO(+)	N.p. 50 mM ammonium acetate	N.p. SFI; 50% MeOH + 5 mM ammonium acetate + 0.1 μM hexakis	TOF	33 differentially accumulated metabolites between MDD and control patients
BNP cleavage peptidoforms in human plasma [228]	CZE(N)	Neutral	10% HAc	Sheathless (CESI 8000)	OT	Monitoring of cleaving recombinant BNP by plasma enzymes
Cyclic peptides for peptide nanotubes [122]	CZE(N)	FS	10 mM carbonate ammonium/ EtOH (50/50)	SFI; 90% EtOH + 2% HAc	Q	Structure and purity control of potential precursors for peptide nanotubes
Highly hydrophobic temporin peptides [123]	NACE	FS	MeOH/ACN/FAc (78/20/2) + 20 mM ammonium hydrogencarbonate	SFI; 2 mM ammonium formate in EtOH	TQ	Fast separation of highly hydrophobic temporin peptides with non-aqueous CE-MS

AAEE: polymerized *N*-acryloylaminoethoxyethanol, **ACE**: affinity CE, **ACEI**: angiotensin-I-converting enzyme, **APFO**: ammonium perfluorooctanoate, **BNP**: B-type natriuretic peptide, **CD**: cyclodextrin, **COPD**: chronic obstructive pulmonary disease, **CS**: chiral selector, **DBS**: dried blood spot, **EtOH**: ethanol, **FAc**: formic acid, **FLEC**: fluorenylethyl-chloroformate, **FS**: fused silica, **IPA**: isopropanol, **MDD**: major depressive disorder, **MeOH**: methanol, **n.p.**: not provided, **N/R**: normal/reversed polarity, **OT**: Orbitrap, **PAM**, polyacrylamide, **Q**: quadrupole, **RNA**: ribonucleic acid, **SFI**: sheath flow interface, **SLE**: systemic lupus erythematosus, **VC**: vancomycin chloride

© 2018 WILEY-VCH Verlag GmbH & Co. KGaA, Weinheim

© 2018 WILEY-VCH Verlag GmbH & Co. KGaA, Weinheim

Table 5. Metabolite analysis and metabolomics (includes papers on research on metabolism, nutrition and disease on microorganisms, cell cultures, plants and mammals as well as humans)

Samples	Mode	Coating	BGE	Interface; sheath liquid	MS	Comments
Yeast [153] *Lactococcus lactis* [156] *O. japonicus* [162]]	CZE(N)	FS	HMT BGE pos. mode	SFI, HMT sheath-liquid 50% MeOH + 5 mM ammonium acetate [229]	TOF	Analysis performed with different commercially available HMT electrolytes and sheath liquid.
Human stem cells [229]	CZE(R)	FS	HMT BGE neg. mode	HMT sheath liquid N.p. [229]		
Corynebacterium glutamicum [157] Mouse serum/plasma [144,145,150], feces [145], luminal [145], arterial [147] and colonic [144], muscle [139] and brain [143] tissue Sheep liver tissue [230] Pork [231] Renal carcinoma cells [232]	CZE(N)	FS	HMT BGE pos. mode	N.p.	TOF	Untargeted metabolomics; Analysis performed with different commercially available HMT electrolytes and sheath liquid.
Human urine [133]	CZE(R)	FS	HMT BGE neg. mode			
Human urine [134] Bovine aortic endothelial cells [233]	CZE(N)	FS	HMT BGE pos. mode	SFI, HMT sheath liquid [134] N.p. [233]	TOF	Analysis in positive mode only
Human aqueous humor [167] Human/Rodent stem cells [126] Human plasma [129] Rodent liver tissue [142]	CZE(N)	FS	0.8 M FAc in 10% MeOH	SFI 50% MeOH [129] 50% MeOH + 1 mM FAc [126,167] 50% MeOH + 0.1 mM FAc [142]	TOF	Identification of 44 [167], 232 [129] and 129 [142] metabolites respectively; Up to ~13,000 variables by LC- and CE-MS [126]
Rodent glioma tissue [146] Rodent muscle tissue [234]	CZE(N)	FS	1 M FAc	SFI 50% MeOH + 0.1 μM hexakis [146,159,161] HMT sheath liquid [234]	TOF	Identification of 106 [146], 412 [159] and 367 [161] metabolites Influence of taurine on carbohydrate metabolism [234]
Tobacco leaves [159,161]	CZE(R)	FS	50 mM ammonium acetate			
Human saliva [136]	CZE(N)	FS	1 M FAc	SFI, 50% MeOH + 0.1% reserpine/hexakis	TOF	Identification of 137 [136], 183 [149], 94 [152] and 110 [119] metabolites respectively; Analysis of metabolites of the urea cycle, TCA pathway and amino acid production [235]
Rodent plasma, urine, feces [149] Rodent feces [152] *In vitro* liver model [235] Human tumor tissue [119] Human serum/plasma [236]	CZE(R)	Cationic coating	50 mM ammonium acetate	SFI, 50% MeOH + 5 mM ammonium acetate + 0.1 μM reserpine/hexakis		

(*Continued*)

Table 5. Continued

Samples	Mode	Coating	BGE	Interface; sheath liquid	MS	Comments
Rumex leafs [160] Head lettuce [237] Gentian leafs [138]	CZE(N)	FS	1 M FAc	SFI; 50% MeOH + 0.1% FAc	TOF [138, 160]; Q [164]N.p. [237]	Targeted and quantitative analysis of 50 [160, 237] and 57 [138, 164] metabolites
Mushrooms [164]	CZE(R)	PEG	20 mM ammonium acetate	SFI; 50% MeOH + 5 mM ammonium acetate		
Yeast [168]	CZE(N)	FS	1 M FAc	SFI	TOF	Integration of LC- and CE-MS data [168]
HL-60 cells [238, 239]				60% IPA + 0.05% FAc [168]		Identification of 50 [238] and 94 [152],
Rodent feces [152]				50% MeOH +0.1% FAc [238, 239]		quantification of 94 metabolites [128]
Human Plasma [128]				HMT sheath liquid [152]		Determination of GSH/GSSG ratio [239]
Flaxseeds [240]				50% MeOH + 0.5 μM reserpine [128]		^{13}C-labeled amino acid analysis [240]
				50% MeOH + 2.5 μM ammonium acetate [240]		
Human sweat [137]	CZE(N)	FS	1 M FAc in 15% can	SFI; 60% MeOH + 0.1% FAc	TOF	Identification of 64 metabolites
	CZE(R)	FS	50 mM ammonium hydrogencarbonate	SFI;50% MeOH		
Human urine [111]	CZE(R)	PAM	50 mM ammonium acetate + 25 mM VC (CS) (pH 4.5)	SFI; 50% MeOH + 0.5% ammonium hydroxide	TQ	Enantioseparation of D/L-hydroxyglutaric acid in urine
Human urine [131]	CZE(R)	FS	50 mM ammonium hydrogencarbonate	SFI; 50% MeOH	TOF	MSI and fast separation of 30 anionic metabolites
Human urine [135]	CZE(R)	FS	20 mM ammonium acetate in 10% MeOH	SFI; 50% IPA + 0.25% FAc	Q	Separation of 3 organic acids in human urine
Plant extract [163]	NACE, CZE(N)	FS	20 mM ammonium acetate in MeOH/ACN (80/20)	SFI; 0.2 mM ammonium acetate in EtOH	TQ	Successful separation and quantification of three anthraquinones by NACE
Human urine [132]	CZE(N)	FS	250 mM FAc in 20% can	SFI; 250 mM FAc in 20% ACN	TOF	Highly reproducible long-term measurements
Zebrafish embryos [241]	CZE(N)	AAEE	0.75 M HAc, 0.25 M FAc	SFI; 50% IPA + 0.1% FAc	TOF	Significance of spermidine in early development of zebra fish
Human plasma [127]	CZE(N)	FS	3.95% FAc	SFI; 50% MeOH + 0.1 μM hexakis	TOF	Identification of 228 metabolites
	CZE(R)	FS	50 mM ammonium acetate	SFI; 50% MeOH + 0.1 μM hexakis		
Cyanobacteria [155]	CZE(N)	PEG	20 mM ammonium acetate	SFI; 50% MeOH + 5 mM ammonium acetate +0.1 μM hexakis	Q	18 targeted metabolites
Human serum/plasma [130, 166] Yeast [158]	N.p.	N.p.	N.p.	N.p.	TOF/Q	No method parameters given

AAEE: polymerized *N*-acryloylaminoethoxyethanol, **CS**: chiral selector, **EtOH**: ethanol, **FAc**: formic acid, **FS**: fused silica, **GSH/GSSG**: oxidized/reduced glutathione, **HAc**: acetic acid, **IPA**: isopropanol, **MeOH**: methanol, **n.p.**: not provided, **N/R**: normal/reversed polarity, **PEG**: polyethylene glycol, **Q**: quadrupole, **SFI**: sheath flow interface, **TCA**: tricarboxylic acid, **VC**: vancomycin chloride

© 2018 WILEY-VCH Verlag GmbH & Co. KGaA, Weinheim

Table 6. Pharmaceutical and clinical applications (publications on identification of active substances in drug formulations and biological fluids as well as basic pharmaceutical research)

Analytes/samples	Mode	Coating	BGE[a)]	Interface; sheath liquid	MS	Comments	Ref.
Six commercial drugs in their formulation	CZE(N)	FS	10 mM ammonium acetate in 5% MeOH	SFI; 50% MeOH + 5 mM ammonium acetate	TQ	Determination and quantification of drug and multidrug doses	[176]
Azathioprine and metabolites in urine	CZE(N)	FS	10 mM ammonium acetate in 5% MeOH	SFI; 50% MeOH + 5 mM ammonium acetate	TQ	Determination of azathioprine and metabolites in urine samples	[169]
Varenicline in urine	CITP-CZE	MHEC	20 mM HAc	SFI 50% MeOH + 0.1% HAc	TQ	Comparison and validation of CITP-CZE-UV and CZE-MS method	[170]
5-nitroimidazoles and metabolites in urine	CZE(N)	FS	1 M FAc	SFI; 60 % IPA + 0.2 % HAc	IT	Comparison of MEKC and CZE method	[171]
Vildagliptin	CZE(N)	FS	0.25 mM ammonium formate	N.p. 50% MeOH + 0.25% FAc	TQ	Pharmacokinetic study of vildagliptin in rats	[172]
Decapeptide as β-secretase inhibitor	CZE(N)	FS	12.5% HAc	SFI; 50% MeOH	TOF	Study of enzyme kinetics (ß-secretase) treated with inhibitors; determination of proteolytic peptides	[177]
Metal-based anticancer agents: Cisplatin and RAPTA-C (Ru), metabolites in cell culture medium	CZE(N)	PVP/PB	PVP: 25 mM phosphate (pH 7.4) PB: 50 mM FAc	SFI; 20 mM NH4Ac, 20 μg/L Ge, Sc, Re (IS)	ICP-MS	Metabolites of RAPTA-C and cisplatin in cell culture medium. PVP coating better than PB coating. The presence of cancer cells had impact on the species distribution of anticancer metal complexes	[179]
Ru(III) anticancer agent	CZE(N)	FS	10 mM Phosphate, 4 mM NaCl, pH 6.0"	SFI; 10% BGE, 20 μg/L Ge (IS)	ICP-MS	Interaction with proteins in the presence of other cytosol components (e.g. amino acids). Two different approaches: 1) in-capillary reaction, 2) offline with sample cleanup.	[183]
NKP-1339, RM175 and RAPTA-C	CZE(N)	FS	25 mM ammonium carbonate	SFI; 25% IPA, 25% MeOH + 0.2% FAc + 0.5% NBA	TOF	Analysis of activation mechanism and binding preferences of three ruthenium anticancer agents	[181]
RM175, Cisplatin	CZE(N)	FS	25 mM ammonium carbonate	SFI; 25% IPA, 25% MeOH + 0.2% FAc + 0.5% NBA	TOF	Binding characterization and quantification of metal-based anticancer agents to Protein/DNA	[180]
Ru(III) complex anticancer drug, in different mouse tissue	CZE(R)	PB	N.p.	SFI; 50 mM HAc, 20 μg/L Ge (IS)	ICP-MS	Determination of tissue distribution of anticancer drug candidate KP-1339/IT139. High affinity to proteins confirmed	[182]
Ru(III) anticancer drug	CZE(N)	FS	10 mM NaH2PO4, 10 mM Na2HPO4, 4 mM NaCl (pH 6.0)	SFI; 10% BGE (pH 6.0), 20 μg/L Ge (IS)	ICP-MS	CZE-ICP-MS used for characterization of metallodrug-DNA binding complexes	[242]
Benzodiazepines in blood serum	NACE	SMIL	20 mM ammonium acetate + 100 mM TFA in ACN	SFI; 50% MeOH + 0.2% FAc	TQ	Determination and quantification of benzodiazepines with NACE	[173]
Amphetamines in natural weight loss pills and dietary supplements	CZE(N)	PVA	0.1 M FAc	SFI; 50% MeOH + 20 mM FAc	TQ	Determination and quantification of amphetamines after QuEChERS extraction	[174]
DoA in urine	MSI-CZE(N)	FS	1 M FAc in 13% ACN	SFI; 60% MeOH + 0.1% FAc	TOF	Detection and identification of more than 50 DoA in 10 different injected samples by MSI	[175]
Enolase digest	CZE(N)	FS	0.1% HAc + 0.1% cationic polymer	Sheathless interface	IT	Analysis of a protein digest in ~1 min with short capillaries	[178]
β-carboline alkaloids in algae	CZE(N)	FS	10 mM ammonium acetate in 10% MeOH	SFI; 60% IPA	TOF	Preconcentration of about 1000-times with online SPE CE-MS	[184]
Pu(IV) chelating agents	CZE(N)	FS	Nitric acid medium, not further specified	SFI: 2% nitric acid in 10% EtOH	ICP-MS	Stability constants related to complexation of actinoides with chelating agents determined under different conditions.	[243]

a) **Mode: all CZE**

DoA: Drugs of abuse, **EtOH**: ethanol, **FAc**: formic acid, **FS**: fused silica, **HAc**: acetic acid, **IPA**: isopropanol, **IS**: internal standard, **MeOH**: methanol, **MHEC**: methyl hydroxyethyl cellulose, **NBA**: n-butanol, **N/R**: normal/reversed polarity, **PB**: polybrene, **SFI**: sheath flow interface, **SMIL**: successive multiple ionic-polymer layer

© 2018 WILEY-VCH Verlag GmbH & Co. KGaA, Weinheim

Table 7. Environmental and food analysis (CE-MS methods for the analysis of environmental and food samples)

Analytes/samples	Mode[a)]	Coating	BGE	Interface; sheath liquid	MS	Comments	Ref.
Monosaccharides in coffee	N	FS	500 mM TEA	SFI; 50% MeOH + 10 mM TEA	TQ	Adulteration analysis of coffee by monosaccharides	[186]
β-*N*-methylamino-L-alanine in cycad, lobster, and mussel	N	FS	5 M FAc in 10% can	50% MeOH + 0.1% FAc	TQ	LOD = 0.8 ng/mL / 16 ng/g	[187]
Tetracycline and quinolone antibiotics in milk	N	FS	75 mM ammonium acetate + 2.5 mM EDTA	SFI; 70% MeOH + 0.1% FAc +purine/hexakis	TOF	Validated method with LOQ = 1.5-9.6 μg/kg	[188]
Fatty acids in coffee and cheese	N	FS	30 mM ammonium formate in 40% can	SFI; 250 μM ion-pairing reagent in 50% MeOH	TOF	Evaluation of ion pairing reagents as addition for the sheath liquid for determination of fatty acids	[190]
Benzimidazoles in meat	N	FS	0.5 M FAc	SFI; 50% EtOH + 0.5% FAc	IT	LOD < 3μg/kg	[189]
Zn binding ligands in Goji berries	N	FS	20 mM ammonium formate pH 9.0	SFI; ESI: 50% MeOH + 5 mM ammonium formate ICP: 2 mM HEPES, GE (IS)	ESI-TQ ICP-MS	CE-ICP-MS provides information about presence of Zn species and CE-ESI-TQ-MS enables identification.	[191]
Saxitoxin in seafood	N	FS	20 mM NaH_2PO_4, 5 mM $Na_2B_4O_7$, pH 6.0	SFI, SL n.p.	ICP-MS	Saxitoxin quantification by Eu^{3+} chelate labeling	[192]
^{13}C-labeled amino acids in flaxseeds	N	FS	1 M FAc	SFI; 2.5μM ammonium acetate in 50% MeOH	TOF	Metabolic pathway analysis in flaxseeds	[240]
Organic acids in Japanese sake	N	FS	N.p. (HMT)	N.p. (HMT)	TOF		[244]
Nucleosides and nucleotide phosphates in fish, meat, fruits, yogurt	N	FS	76 mM HFIP	SFI; 1.6% HFIP	Q	HFIP improved both separation (in BGE) and sensitivity (in SL), LODs: mid ng/mL-range	[245]
Organic acids in red wine	R	PB	50 mM ammonium acetate	SFI; 1% FAc	TOF	Profiling of read vines at the low mM-level of organic acids; LOQ = 3-107 μM	[246]
Fluoroquinolone in environmental water	N	FS	50 mM ethylendiamin-FAc	SFI; 50% MeOH +0.1% FAc	IT	Determination of eight typical fluoroquinolone after IAE	[195]
N-containing compounds (amines, amino acids) in soil	N	FS	2 M FAc in 30% MeOH	SFI; 50% MeOH + 0.1% FAc	IT	63 compounds determined based on standards/databases	[196–198]
Naphthenic acids (diamine derivatization) in oil sands process-affected water	N	FS	2% FAc in 30% MeOH	'Junction at the tip interface' with modifier solution identical to BGE delivered at 100 nL/min	TOF	Naphthenic acid derivatized with primary-tertiary diamine	[199, 200]
Pu in aqueous samples	N	FS	1 M HAc	SFI; 2% nitric acid in 10% MeOH	ICP-MS	Oxidation state distribution of Pu by CE-ICP-MS under different solvent conditions	[201]
Eu^{3+} and UO_2^{2+} complexes with NOM from different sources	N	FS	100 mM HAc, 10 mM sodium acetate, 200 μg/L Cs (IS), pH 3.7	SFI; 2% nitric acid, 4 μg/L Ho (IS)	ICP-MS	Determination complex stability constants of U(VI) and Eu(III) with NOM	[202, 203]

(*Continued*)

© 2018 WILEY-VCH Verlag GmbH & Co. KGaA, Weinheim

Table 7. Continued

Analytes/samples	Mode[a)]	Coating	BGE	Interface; sheath liquid	MS	Comments	Ref.
U(VI) interactions with calcium phosphate-binding proteins	R/N	FS HPC	10 mM TRIS, 15 mM NaCl, pH 7.4	SFI; FS: 1 mM nitric acid HPC: 5 mM tris	ICP-MS	Indication that the presence of U(VI) causes a slower growth rate of protein particles by forming complexes	[204]
Hydroxy-triazines in water	Moving boundary ITP	FS	LE: 10 mM ammonium acetate TE: 10 mM HAc,	50% MeOH + 5 mM HAc + 3 mM ammonium	Q	LOD < 0.5 nM (0.1 ng/mL)	[193]
Sulfonamides in water	Inverse EMD	FS	LE: 15.2 mM maleic acid, 21.7 mM 2,6-lutidine TE: 2 mM maleic acid, 27.6 mM 2,6-lutidine	50% MeOH + 5 mM HAc, 3 mM 2,6-lutidine	Q	LOD: 3 nM (0.8 ng/mL)	[194]
Pu complex with transferrin	N	Neutral Coating	80 mM NaCl, 57 mM MES, 1 μM NTA, pH 6.0	SFI; 2% nitric acid in 10% EtOH	ICP-MS	Binding constant for Pu to transferrin by CZE-ICP-MS	[205]
Pb species in algae	R	FS	70 mM boric acid, 17.5 mM $Na_2B_4O_7$, pH 8.9	SFI; 5% MeOH	ICP-MS	Separation and quantification of three lead species. LOD in lower ppt range	[247]
MeHg in natural water samples	N	FS	50 mM boric acid 3, 12.5 mM $Na_2B_4O_7$, pH 9.2	SFI; SL n.p.	ICP-MS	LOD of 0.084 pg/mL	[248]

a) **Mode: all CZE**
EMD: electromigration dispersion, **EtOH**: ethanol, **FAc**: formic acid, **FS**: fused silica, **HAc**: acetic acid, **HFIP**: hexafluoro-2-propanol, **HPC**: hydroyxypropyl cellulose **IAE**: immunoaffinity enrichment, **LE**: leading electrolyte, **MeHg**: Methylmercury, **MeOH**: methanol, **n.p.**: not provided, **N/R**: normal/reversed polarity, **NTA**: nitrilotriacetic acid, **PB**: polybrene, **ppt**: parts per trillion, **Q**: quadrupole, **SF**: sector field, **SFI**: sheath flow interface, **SL**: sheath liquid, **TE**: terminating electrolyte, **TEA**: trimethylamine

Table 8. Nanoparticles

Analytes	Mode[a)]	Coating	BGE	Interface; sheath liquid	MS	Comments	Ref.
AuNP	N	FS	70 mM SDS, 10 mM CAPS, pH 10	SFI; 2% nitric acid, 10 μg/L In (IS)	SP-ICP-MS	Detection of particles down to 10 μm. Potential use in high-throughput fractionation	[206]
AgNP	N	FS	60 mM SDS, 10 mM CAPS, 10 μg/L Cs, pH 10	SFI; 2% nitric acid, 10 μg/L In (IS)	SP-ICP-MS	AgNPs separated by size	[207,208]
AuNP	N	FS	10 mM CHES, 70 mM SDBS, pH 10	SFI; 1% nitric acid, 10% IPA	ICP-MS	Influence of different matrices on separation performance	[209]
AuNP	N	FS	40 mM HEPES, pH 7.4	SFI; 10% BGE, 20 μg/L Ge (IS)	ICP-MS	Determination of stoichiometric composition of protein corona of AuNPs	[210]
AuNP	N	FS	10 mM PIPES, pH 7.4 (rAuNPs)	SFI; 10% BGE, 20 μg/L Ge (IS)	ICP-MS	Optimization of CE method for rod-shaped AuNPs	[211]
AuNP	N	FS	40 mM HEPES, pH 7.4 (sAuNPs) 10 mM PIPES, pH 7.4 (rAuNPs)	SFI; 10% BGE, 20 μg/L Ge (IS)	ICP-MS	Interaction of rod- and spherical-shaped AuNPs with different serum proteins evaluated	[212]
AuNP	N	FS	40 mM HEPES, pH 7.4	SFI; 10% BGE, 20 μg/L Ge (IS)	ICP-MS	Interaction of AuNPs with proteins in artificial cytosol (normal and cancer)	[213]

a) **Mode: all CZE**
CAPS: *N*-cyclohexyl-3-aminopropanesulfonic acid, **FS**: fused silica,, **IPA**: isopropanol, **IS**: internal standard, **N/R**: normal/reversed polarity, **PIPES**: piperazine-*N*,*N*-bis(2-ethanesulfonic acid), **SDBS**: sodium dodecylbenzenesulfonate, **rAUNP**: rod-shaped AuNP, **sAUNP**: spherical-shaped AuNP **SFI**: sheath flow interface

© 2018 WILEY-VCH Verlag GmbH & Co. KGaA, Weinheim

Table 9. Single cell analysis

Analytes/samples	Mode	Coating	BGE	Interface; sheath liquid	MS	Performance/ Result	Ref.
Single cell metabolite extracts (*Xenopus* embryo)	CZE(N)	FS	1% FAc	SFI; 50% MeOH + 0.1% FAc	TOF	10 of 55 identified metabolites were differentially accumulated in right and left embryotic cells of Xenopus	[217]
Single cells of *Xenopus* embryos, tryptic digestion	CZE(N)	FS	1M FAc in 25% can	SFI; 0.1% FAc in 50% MeOH	TOF	Identification and quantification of 350 protein groups within a single cell	[218]
Single cell metabolite extracts (Xenopus embryo)	CZE(N)	FS	1% FAc	SFI; 0.1% FAc in 50% MeOH	TOF	Microprobe sampling enables improved metabolite profiling using less sample	[219]
Neuronal protein digest	CZE(N)	FS	1 M FAc in 50% can	Nano-SFI; 50% MeOH + 0.1% FAc	OT	Reversed-phase fractionation; identification of 225 protein groups (623 peptide IDs)	[22]
Single pancreatic rat cells on a MALDI target plate	CZE(N)	FS	1% FAc	SFI; 0.1% FAc in 50% MeOH	CE-TOF + MALDI	Combined characterization of lipids, peptides and metabolites by MALDI-MS and CE-MS of single cells	[29]

FAc: formic acid, **FS**: fused silica, **MeOH**: methanol, **N/R**: normal/reversed polarity, **OT**: Orbitrap, **SFI**: sheath flow interface

6 References

[1] Klepárník, K., *Electrophoresis* 2015, *36*, 159–178.

[2] Týčová, A., Ledvina, V., Klepárník, K., *Electrophoresis* 2017, *38*, 115–134.

[3] Jie, M., Mao, S., Li, H., Lin, J.-M., *Chin. Chem. Lett.* 2017, *28*, 1625–1630.

[4] Pedde, R. D., Li, H., Borchers, C. H., Akbari, M., *Trends Biotechnol.* 2017, *35*, 954–970.

[5] Bonvin, G., Schappler, J., Rudaz, S., *J. Chromatogr. A* 2012, *1267*, 17–31.

[6] Lindenburg, P. W., Haselberg, R., Rozing, G., Ramautar, R., *Chromatographia* 2015, *78*, 367–377.

[7] Moini, M., *Anal. Chem.* 2007, *79*, 4241–4246.

[8] Nguyen, Tam T. T. N., Petersen, N. J., Rand, K. D., *Anal. Chim. Acta* 2016, *936*, 157–167.

[9] Johnson, R. T., To, N. H., Stobaugh, J. F., Lunte, C. E., *Chromatographia* 2017, *80*, 1061–1067.

[10] Hirayama, A., Abe, H., Yamaguchi, N., Tabata, S., Tomita, M., Soga, T., *Electrophoresis* 2018, *39*, 1382–1389.

[11] Týčová, A., Foret, F., *J. Chromatogr. A* 2015, *1388*, 274–279.

[12] Týčová, A., Vido, M., Kovarikova, P., Foret, F., *J. Chromatogr. A* 2016, *1466*, 173–179.

[13] Kammeijer, G. S. M., Kohler, I., Jansen, B. C., Hensbergen, P. J., Mayboroda, O. A., Falck, D., Wuhrer, M., *Anal. Chem.* 2016, *88*, 5849–5856.

[14] Jarvas, G., Fonslow, B., Yates, J. R. III, Foret, F., Guttman, A., *J. Chromatogr. Sci.* 2017, *55*, 47–51.

[15] Jarvas, G., Szigeti, M., Guttman, A., *J. Sep. Sci.* 2018, *11*, 2473–2478.

[16] Sun, L., Zhu, G., Zhang, Z., Mou, S., Dovichi, N. J., *J. Proteome Res.* 2015, *14*, 2312–2321.

[17] Sarver, S. A., Schiavone, N. M., Arceo, J., Peuchen, E. H., Zhang, Z., Sung, L., Dovichi, N. J., *Talanta* 2017, *165*, 522–525.

[18] Höcker, O., Montealegre, C., Neusüß, C., *Anal. Bioanal. Chem.* 2018, *410*, 5265–5275.

[19] Gonzalez-Ruiz, V., Codesido, S., Far, J., Rudaz, S., Schappler, J., *Electrophoresis* 2016, *37*, 936–946.

[20] Gonzalez-Ruiz, V., Codesido, S., Rudaz, S., Schappler, J., *Electrophoresis* 2018, *39*, 853–861.

[21] Choi, S. B., Zamarbide, M., Manzini, M. C., Nemes, P., *J. Am. Soc. Mass Spectrom.* 2017, *28*, 597–607.

[22] Choi, S. B., Lombard-Banek, C., Muñoz-LLancao, P., Manzini, M. C., Nemes, P., *J. Am. Soc. Mass Spectrom.* 2018, *29*, 913–922.

[23] Fang, P., Pan, J.-Z., Fang, Q., *Talanta*. 2018, *180*, 376–382.

[24] Flaherty, R. J., Sarver, S. A., Sun, L., Brownell, G. A., Go, D. B., Dovichi, N. J., *J. Am. Soc. Mass Spectrom.* 2017, *28*, 247–252.

[25] Beutner, A., Scherer, B., Matysik, F.-M., *Talanta* 2018, *183*, 33–38.

[26] Mendonca Francisco, K. J., do Lago, C. L., *Electrophoresis* 2016, *37*, 1718–1724.

© 2018 WILEY-VCH Verlag GmbH & Co. KGaA, Weinheim

[27] Biacchi, M., Bhajun, R., Saïd, N., Beck, A., François, Y. N., Leize-Wagner, E., *Electrophoresis* 2014, *35*, 2986–2995.

[28] Biacchi, M., Said, N., Beck, A., Leize-Wagner, E., Francois, Y.-N., *J. Chromatogr. A* 2017, *1498*, 120–127.

[29] Comi, T. J., Makurath, M. A., Philip, M. C., Rubakhin, S. S., Sweedler, J. V., *Anal. Chem*. 2017, *89*, 7765–7772.

[30] Yang, G., Xu, J., Zheng, J., Xu, X., Wang, W., Xu, L., Chen, G., Fu, F., *Talanta* 2009, *78*, 471–476.

[31] Chen, J., Fu, F., Wu, S., Wang, J., Wang, Z., *J. Sep. Sci*. 2017, *40*, 3898–3904.

[32] Shuai, P.-Y., Yang, X.-J., Qiu, Z.-Q., Wu, X.-H., Zhu, X., Pokhrel, G. R., Fu, Y.-Y., Ye, H.-M., Lin, W.-X., Yang, G.-D., *J. Sep. Sci*. 2016, *39*, 3239–3245.

[33] Holtkamp, H. U., Morrow, S. J., Kubanik, M., Hartinger, C. G., *J. Biol. Inorg. Chem*. 2017, *22*, 789–798.

[34] Cheng, H., Liu, J., Xu, Z., Wang, Y., Ye, M., *J. Chromatogr. A* 2016, *1461*, 198–204.

[35] Chaudhari, S., Chaudhari, K., Kim, S., Khan, F., Lee, J., Thundat, T., *Sci. Rep*. 2017, *7*.

[36] Zhang, Y., Ai, W., Bai, Y., Zhou, Y., Wen, L., Zhang, X., Liu, H., *Anal. Bioanal. Chem*. 2016, *408*, 8655–8661.

[37] Sydes, D., Kler, P. A., Hermans, M., Huhn, C., *Electrophoresis* 2016, *37*, 3020–3024.

[38] Kohl, F. J., Montealegre, C., Neusüß, C., *Electrophoresis* 2016, *37*, 954–958.

[39] Hühner, J., Neusüß, C., *Anal. Bioanal. Chem*. 2016, *408*, 4055–4061.

[40] Hühner, J., Jooß, K., Neuesuss, C., *Electrophoresis* 2017, *38*, 914–921.

[41] Montealegre, C., Neusüß, C., *Electrophoresis* 2018, *39*, 1151–1154.

[42] Jooß, K., Hühner, J., Kiessig, S., Moritz, B., Neusüß, C., *Anal. Bioanal. Chem*. 2017, *409*, 6057–6067.

[43] Neuberger, S., Jooß, K., Ressel, C., Neusüß, C., *Anal. Bioanal. Chem*. 2016, *408*, 8701–8712.

[44] Bertoletti, L., Schappler, J., Colombo, R., Rudaz, S., Haselberg, R., Dominguez-Vega, E., Raimondi, S., Somsen, G. W., Lorenzi, E. de, *Anal. Chim. Acta* 2016, *945*, 102–109.

[45] Marie, A.-L., Dominguez-Vega, E., Saller, F., Plantier, J.-L., Urbain, R., Borgel, D., Thuy Tran, N., Somsen, G. W., Taverna, M., *Anal. Chim. Acta* 2016, *947*, 58–65.

[46] Belov, A. M., Viner, R., Santos, M. R., Horn, D. M., Bern, M., Karger, B. L., Ivanov, A. R., *J. Am. Soc. Mass Spectrom*. 2017, *28*, 2614–2634.

[47] Mironov, G. G., Clouthier, C. M., Akbar, A., Keillor, J. W., Berezovski, M. V., *Nat. Chem. Biol*. 2016, *12*, 918.

[48] Han, M., Pearson, J. T., Wang, Y., Winters, D., Soto, M., Rock, D. A., Rock, B. M., *Anal. Biochem*. 2017, *539*, 118–126.

[49] Tengattini, S., Dominguez-Vega, E., Temporini, C., Terreni, M., Somsen, G. W., *Anal. Bioanal. Chem*. 2016, *408*, 6123–6132.

[50] Lubeckyj, R. A., McCool, E. N., Shen, X., Kou, Q., Liu, X., Sun, L., *Anal. Chem*. 2017, *89*, 12059–12067.

[51] Sánchez-Hernández, L., Montealegre, C., Kiessig, S., Moritz, B., Neusüß, C., *Electrophoresis* 2017, *38*, 1044–1052.

[52] Zhu, G., Sun, L., Dovichi, N. J., *J. Sep. Sci*. 2017, *40*, 948–953.

[53] Páger, C., Biherczová, N., Ligetvári, R., Berkics, B. V., Pongrácz, T., Sándor, V., Bufa, A., Poór, V., Vojs Staňová, A., Kilár, F., *J. Sep. Sci*. 2017, *40*, 4825–4834.

[54] Dada, O. O., Zhao, Y., Jaya, N., Salas-Solano, O., *Anal. Chem*. 2017, *89*, 11227–11235.

[55] Dada, O. O., Zhao, Y., Jaya, N., Salas-Solano, O., *Anal. Chem*. 2017, *89*, 11236–11242.

[56] Chen, H., Shi, P., Fan, F., Tu, M., Xu, Z., Xu, X., Du, M., *J. Chromatogr. B Analyt. Technol. Biomed. Life Sci*. 2018, *1084*, 150–157.

[57] Reich, M., Dacheva, I., Nobl, M., Siwy, J., Schanstra, J. P., Mullen, W., Koch, F. H. J., Kopitz, J., Kretz, F. T. A., Auffarth, G. U., Koss, M. J., *PLoS One* 2016, *11*, e0158001.

[58] Boley, D. A., Zhang, Z., Dovichi, N. J., *J. Chromatogr. A* 2017, *1523*, 123–126.

[59] Faserl, K., Sarg, B., Sola, L., Lindner, H. H., *Proteomics* 2017, *17*, 1700310.

[60] Zhang, Z., Zhu, G., Peuchen, E. H., Dovichi, N. J., *Microchimica Acta* 2017, *184*, 921–925.

[61] Chen, D., Shen, X., Sun, L., *Analyst* 2017, *142*, 2118–2127.

[62] Sarg, B., Faserl, K., Lindner, H. H., *Proteomics* 2017, *17*, 1700269.

[63] Faserl, K., Sarg, B., Maurer, V., Lindner, H. H., *J. Chromatogr. A* 2017, *1498*, 215–223.

[64] Dominguez-Vega, E., Vijlder, T. de, Romijn, E. P., Somsen, G. W., *Anal. Chim. Acta* 2017, *982*, 122–130.

[65] Faserl, K., Sarg, B., Gruber, P., Lindner, H. H., *Electrophoresis* 2018, *39*, 1208–1215.

[66] Krokhin, O. V., Anderson, G., Spicer, V., Sun, L., Dovichi, N. J., *Anal. Chem.* 2017, *89*, 2000–2008.

[67] Gusenkov, S., Stutz, H., *Electrophoresis* 2018, *39*, 1190–1200.

[68] Yan, X., Sun, L., Zhu, G., Cox, O. F., Dovichi, N. J., *Proteomics* 2016, *16*, 2945–2952.

[69] Chen, D., Shen, X., Sun, L., *Anal. Chim. Acta* 2018, *1012*, 1–9.

[70] McCool, E. N., Lubeckyj, R. A., Shen, X., Chen, D., Kou, Q., Liu, X., Sun, L., *Anal. Chem.* 2018, *90*, 5529–5533.

[71] Gahoual, R., Beck, A., Leize-Wagner, E., Francois, Y.-N., *J. Chromatogr. B Analyt. Technol. Biomed. Life Sci.* 2016, *1032*, 61–78.

[72] Zhang, Z., Albanetti, T., Linkous, T., Larkin, C. J., Schoner, R., McGivney, J. B., Dovichi, N. J., *Electrophoresis* 2017, *38*, 401–407.

[73] Dai, J., Lamp, J., Xia, Q., Zhang, Y., *Anal. Chem.* 2018, *90*, 2246–2254.

[74] Váradi, C., Mittermayr, S., Millán-Martín, S., Bones, J., *Anal. Bioanal. Chem.* 2016, *408*, 8691–8700.

© 2018 WILEY-VCH Verlag GmbH & Co. KGaA, Weinheim

[75] Snyder, C. M., Zhou, X., Karty, J. A., Fonslow, B. R., Novotny, M. V., Jacobson, S. C., *J. Chromatogr. A* 2017, *1523*, 127–139.

[76] Kammeijer, G. S. M., Jansen, B. C., Kohler, I., Heemskerk, A. A. M., Mayboroda, O. A., Hensbergen, P. J., Schappler, J., Wuhrer, M., *Sci. Rep.* 2017, *7*, 3733.

[77] Kammeijer, G. S. M., Nouta, J., La Rosette, J. J. M. C. H. de, Reijke, T. M. de, Wuhrer, M., *Anal. Chem.* 2018, *90*, 4414–4421.

[78] Qu, Y., Sun, L., Zhu, G., Zhang, Z., Peuchen, E. H., Dovichi, N. J., *Talanta* 2018, *179*, 22–27.

[79] Qu, Y., Sun, L., Zhang, Z., Dovichi, N. J., *Anal. Chem.* 2018, *90*, 1223–1233.

[80] Giorgetti, J., D'Atri, V., Canonge, J., Lechner, A., Guillarme, D., Colas, O., Wagner-Rousset, E., Beck, A., Leize-Wagner, E., François, Y.-N., *Talanta* 2018, *178*, 530–537.

[81] Mancera-Arteu, M., Giménez, E., Benavente, F., Barbosa, J., Sanz-Nebot, V., *J. Proteome Res.* 2017, *16*, 4166–4176.

[82] Lin, L., Liu, X., Zhang, F., Chi, L., Amster, I. J., Leach, F. E., Xia, Q., Linhardt, R. J., *Anal. Bioanal. Chem.* 2017, *409*, 411–420.

[83] Sanderson, P., Stickney, M., Leach, F. E. 3., Xia, Q., Yu, Y., Zhang, F., Linhardt, R. J., Amster, I. J., *J. Chromatogr. A* 2018, *1545*, 75–83.

[84] Fayad, S., Nehme, R., Langmajerova, M., Ayela, B., Colas, C., Maunit, B., Jacquinet, J.-C., Vibert, A., Lopin-Bon, C., Glatz, Z., Morin, P., *Anal. Chim. Acta* 2017, *951*, 140–150.

[85] Cieslarova, Z., Lopes, F. S., do Lago, C. L., Franca, M. C. Jr., Colnaghi Simionato, A. V., *Talanta* 2017, *170*, 63–68.

[86] Forteschi, M., Zinellu, A., Assaretti, S., Mangoni, A. A., Pintus, G., Carru, C., Sotgia, S., *Anal. Bioanal. Chem.* 2016, *408*, 7505–7512.

[87] Umehara, H., Numata, S., Watanabe, S.-y., Hatakeyama, Y., Kinoshita, M., Tomioka, Y., Nakahara, K., Nikawa, T., Ohmori, T., *Sci. Rep.* 2017, *7*, 4855.

[88] Bennuru, S., Lustigman, S., Abraham, D., Nutman, T. B., *Mol. Biochem. Parasitol.* 2017, *215*, 58–69.

[89] Miyamoto, T., Hirayama, A., Sato, Y., Koboyashi, T., Katsuyama, E., Kanagawa, H., Miyamoto, H., Mori, T., Yoshida, S., Fujie, A., Morita, M., Watanabe, R., Tando, T., Miyamoto, K., Tsuji, T., Funayama, A., Nakamura, M., Matsumoto, M., Soga, T., Tomita, M., Toyama, Y., *Bone* 2017, *95*, 1–4.

[90] Saiki, S., Hatano, T., Fujimaki, M., Ishikawa, K.-I., Mori, A., Oji, Y., Okuzumi, A., Fukuhara, T., Koinuma, T., Imamichi, Y., Nagumo, M., Furuya, N., Nojiri, S., Amo, T., Yamashiro, K., Hattori, N., *Sci. Rep.* 2017, *7*, 7328.

[91] Asai, Y., Itoi, T., Sugimoto, M., Sofuni, A., Tsuchiya, T., Tanaka, R., Tonozuka, R., Honjo, M., Mukai, S., Fujita, M., Yamamoto, K., Matsunami, Y., Kurosawa, T., Nagakawa, Y., Kaneko, M., Ota, S., Kawachi, S., Shimazu, M., Soga, T., Tomita, M., Sunamura, M., *Cancers (Basel)* 2018, *10*, 43.

[92] Mitsui, T., Kira, S., Ihara, T., Sawada, N., Nakagomi, H., Miyamoto, T., Shimura, H., Yokomichi, H., Takeda, M., *J. Urol.* 2018, *199*, 1312–1318.

[93] Iida, M., Harada, S., Kurihara, A., Fukai, K., Kuwabara, K., Sugiyama, D., Takeuchi, A., Okamura, T., Akiyama, M., Nishiwaki, Y., Suzuki, A., Hirayama, A., Sugimoto, M., Soga, T., Tomita, M., Banno, K., Aoki, D., Takebayashi, T., *Menopause* 2016, *23*, 749–758.

[94] DiBattista, A., McIntosh, N., Lamoureux, M., Al-Dirbashi, O. Y., Chakraborty, P., Britz-McKibbin, P., *Anal. Chem.* 2017, *89*, 8112–8121.

[95] Pero-Gascon, R., Sanz-Nebot, V., Berezovski, M. V., Benavente, F., *Anal. Chem.* 2018, *90*, 6618–6625.

[96] Schönemeier, B., Metzger, J., Klein, J., Husi, H., Bremer, B., Armbrecht, N., Dakna, M., Schanstra, J. P., Rosendahl, J., Wiegand, J., Jäger, M., Mullen, W., Breuil, B., Plentz, R. R., Lichtinghagen, R., Brand, K., Kühnel, F., Mischak, H., Manns, M. P., Lankisch, T. O., *Pancreas* 2016, *45*, 1018–1026.

[97] MacLennan, M. S., Kok, M. G. M., Soliman, L., So, A., Hurtado-Coll, A., Chen, D. D. Y., *J Chromatogr B Analyt Technol Biomed Life Sci* 2018, *1074*, 79–85.

[98] Frantzi, M., van Kessel, K. E., Zwarthoff, E. C., Marquez, M., Rava, M., Malats, N., Merseburger, A. S., Katafigiotis, I., Stravodimos, K., Mullen, W., Zoidakis, J., Makridakis, M., Pejchinovski, M., Critselis, E., Lichtinghagen, R., Brand, K., Dakna, M., Roubelakis, M. G., Theodorescu, D., Vlahou, A., Mischak, H., Anagnou, N. P., *Clin. Cancer Res.* 2016, *22*, 4077–4086.

[99] Belczacka, I., Latosinska, A., Siwy, J., Metzger, J., Merseburger, A. S., Mischak, H., Vlahou, A., Frantzi, M., Jankowski, V., *Sci. Rep.* 2018, *8*, 5227.

[100] Good, D. M., Zürbig, P., Argilés, A., Bauer, H. W., Behrens, G., Coon, J. J., Dakna, M., Decramer, S., Delles, C., Dominiczak, A. F., Ehrich, J. H. H., Eitner, F., Fliser, D., Frommberger, M., Ganser, A., Girolami, M. A., Golovko, I., Gwinner, W., Haubitz, M., Herget-Rosenthal, S., Jankowski, J., Jahn, H., Jerums, G., Julian, B. A., Kellmann, M., Kliem, V., Kolch, W., Krolewski, A. S., Luppi, M., Massy, Z., Melter, M., Neusüß, C., Novak, J., Peter, K., Rossing, K., Rupprecht, H., Schanstra, J. P., Schiffer, E., Stolzenburg, J.-U., Tarnow, L., Theodorescu, D., Thongboonkerd, V., Vanholder, R., Weissinger, E. M., Mischak, H., Schmitt-Kopplin, P., *Mol. Cell. Proteomics* 2010, *9*, 2424–2437.

[101] Currie, G. E., Scholten, B. J. von, Mary, S., Flores Guerrero, J.-L., Lindhardt, M., Reinhard, H., Jacobsen, P. K., Mullen, W., Parving, H.-H., Mischak, H., Rossing, P., Delles, C., *Cardiovasc. Diabetol.* 2018, *17*, 50.

[102] Lindhardt, M., Persson, F., Oxlund, C., Jacobsen, I. A., Zürbig, P., Mischak, H., Rossing, P., Heerspink, H. J. L., *Nephrol. Dial. Transplant.* 2018, *33*, 296–303.

[103] Magalhães, P., Pejchinovski, M., Markoska, K., Banasik, M., Klinger, M., Svec-Billa, D., Rychlik, I., Rroji, M., Restivo, A., Capasso, G., Bob, F., Schiller, A., Ortiz, A., Perez-Gomez, M. V., Cannata, P., Sanchez-Nino, M. D., Naumovic, R., Brkovic, V., Polenakovic, M., Mullen, W., Vlahou, A., Zurbig, P., Pape, L., Ferrario, F., Denis, C., Spasovski, G., Mischak, H., Schanstra, J. P., *Sci. Rep.* 2017, *7*, 16915.

[104] Rossing, K., Bosselmann, H. S., Gustafsson, F., Zhang, Z.-Y., Gu, Y.-M., Kuznetsova, T., Nkuipou-Kenfack, E.,

© 2018 WILEY-VCH Verlag GmbH & Co. KGaA, Weinheim

Mischak, H., Staessen, J. A., Koeck, T., Schou, M., *PLoS One* 2016, *11*, e0157167.

[105] Magalhães, P., Mischak, H., Zürbig, P., *Curr. Opin. Nephrol. Hypertens.* 2016, *25*, 494–501.

[106] Carleo, A., Chorostowska-Wynimko, J., Koeck, T., Mischak, H., Czajkowska-Malinowska, M., Rozy, A., Welte, T., Janciauskiene, S., *Int. J. Chron. Obstruct. Pulmon. Dis.* 2017, *12*, 829–837.

[107] Zhang, Z.-Y., Nkuipou-Kenfack, E., Yang, W.-Y., Wei, F.-F., Cauwenberghs, N., Thijs, L., Huang, Q.-F., Feng, Y.-M., Schanstra, J. P., Kuznetsova, T., Voigt, J.-U., Verhamme, P., Mischak, H., Staessen, J. A., *J. Am. Soc. Hypertens.* 2018, *12*, 438-447.e4.

[108] Pejchinovski, M., Siwy, J., Metzger, J., Dakna, M., Mischak, H., Klein, J., Jankowski, V., Bae, K. T., Chapman, A. B., Kistler, A. D., *Nephrol. Dial. Transplant.* 2017, *32*, 487–497.

[109] Martín-Pozuelo, G., González-Barrio, R., Barberá, G. G., Albalat, A., García-Alonso, J., Mullen, W., Mischak, H., Periago, M. J., *Int. J. Mol. Sci.* 2016, *17*, 17111789.

[110] Pejchinovski, M., Siwy, J., Mullen, W., Mischak, H., Petri, M. A., Burkly, L. C., Wei, R., *Lupus* 2018, *27*, 6–16.

[111] Švidrnoch, M., Přibylka, A., Bekárek, V., Ševčík, J., Smolka, V., Maier, V., *J. Chromatogr. A* 2016, *1467*, 383–390.

[112] Ohshima, M., Sugahara, K., Kasahara, K., Katakura, A., *Oncol. Rep.* 2017, *37*, 2727–2734.

[113] Ishikawa, S., Sugimoto, M., Kitabatake, K., Sugano, A., Nakamura, M., Kaneko, M., Ota, S., Hiwatari, K., Enomoto, A., Soga, T., Tomita, M., Iino, M., *Sci. Rep.* 2016, *6*, 31520.

[114] Ishikawa, S., Sugimoto, M., Kitabatake, K., Tu, M., Sugano, A., Yamamori, I., Iba, A., Yusa, K., Kaneko, M., Ota, S., Hiwatari, K., Enomoto, A., Masaru, T., Iino, M., *Amino Acids* 2017, *49*, 761–770.

[115] Nagata, Y., Hirayama, A., Ikeda, S., Shirahata, A., Shoji, F., Maruyama, M., Kayano, M., Bundo, M., Hattori, K., Yoshida, S., Goto, Y.-i., Urakami, K., Soga, T., Ozaki, K., Niida, S., *Biomark. Res.* 2018, *6*, 5.

[116] Prior, A., Moldovan, R. C., Crommen, J., Servais, A. C., Fillet, M., Jong, G. J. de, Somsen, G. W., *Anal. Chim. Acta* 2016, *940*, 150–158.

[117] Prior, A., Sánchez-Hernández, L., Sastre-Toraño, J., Marina, M. L., Jong, G. J. de, Somsen, G. W., *Electrophoresis* 2016, *37*, 2410–2419.

[118] Fujii, T., Hattori, K., Miyakawa, T., Ohashi, Y., Sato, H., Kunugi, H., *Schizophr. Res.* 2017, *183*, 70–74.

[119] Yamakawa, Y., Kusuhara, M., Terashima, M., Kinugasa, Y., Sugino, T., Abe, M., Mochizuki, T., Hatakeyama, K., Kami, K., Yamaguchi, K., *Biomed. Res.* 2017, *38*, 41–52.

[120] Saito, T., Sugimoto, M., Okumoto, K., Haga, H., Katsumi, T., Mizuno, K., Nishina, T., Sato, S., Igarashi, K., Maki, H., Tomita, M., Ueno, Y., Soga, T., *World J. Gastroenterol.* 2016, *22*, 6224–6234.

[121] Tu, M., Liu, H., Zhang, R., Chen, H., Mao, F., Cheng, S., Lu, W., Du, M., *J. Agric. Food Chem.* 2018, *66*, 4139–4144.

[122] Cortez-Díaz, M. D., d'Orlyé, F., Gutierrez-Granados, S., Leon-Rodriguez, L. M. de, Varenne, A., *Anal. Biochem.* 2016, *502*, 8–15.

[123] Cheng, J., Chen, D. D. Y., *Electrophoresis* 2018, *39*, 1216–1221.

[124] García, A., Godzien, J., López-Gonzálvez, Á., Barbas, C., *Bioanalysis* 2017, *9*, 99–130.

[125] Zhang, W., Hankemeier, T., Ramautar, R., *Curr. Opin. Biotechnol.* 2017, *43*, 1–7.

[126] Mastrangelo, A., Martos-Moreno, G. A., Garcia, A., Barrios, V., Ruperez, F. J., Chowen, J. A., Barbas, C., Argente, J., *Int. J. Obes.* 2016, *40*, 1494–1502.

[127] Liu, S., Wang, L., Hu, C., Huang, X., Liu, H., Xuan, Q., Lin, X., Peng, X., Lu, X., Chang, M., Xu, G., *Sci. Rep.* 2017, *7*, 8150

[128] Harada, S., Hirayama, A., Chan, Q., Kurihara, A., Fukai, K., Iida, M., Kato, S., Sugiyama, D., Kuwabara, K., Takeuchi, A., Akiyama, M., Okamura, T., Ebbels, T. M. D., Elliott, P., Tomita, M., Sato, A., Suzuki, C., Sugimoto, M., Soga, T., Takebayashi, T., *PLoS One* 2018, *13*, e0191230.

[129] Patricia Cala, M., Teresa Agullo-Ortuno, M., Prieto-Garcia, E., Gonzalez-Riano, C., Parrilla-Rubio, L., Barbas, C., Vanesa Diaz-Garcia, C., Garcia, A., Pernaut, C., Adeva, J., Carmen Riesco, M., Javier Ruperez, F., Antonio Lopez-Martin, J., *J. Cachexia Sarcopenia Muscle* 2018, *9*, 348–357.

[130] Yoshikawa, A., Nishimura, F., Inai, A., Eriguchi, Y., Nishioka, M., Takaya, A., Tochigi, M., Kawamura, Y., Umekage, T., Kato, K., Sasaki, T., Ohashi, Y., Iwamoto, K., Kasai, K., Kakiuchi, C., *Psychiatry Clin. Neurosci.* 2018, *72*, 168–179.

[131] Yamamoto, M., Ly, R., Gill, B., Zhu, Y., Moran-Mirabal, J., Britz-McKibbin, P., *Anal. Chem.* 2016, *88*, 10710–10719.

[132] Boizard, F., Brunchault, V., Moulos, P., Breuil, B., Klein, J., Lounis, N., Caubet, C., Tellier, S., Bascands, J.-L., Decramer, S., Schanstra, J. P., Buffin-Meyer, B., *Sci. Rep.* 2016, *6*, 34453.

[133] Yamamoto, H., Sasaki, K., *Electrophoresis* 2017, *38*, 1053–1059.

[134] Shoji, H., Taka, H., Kaga, N., Ikeda, N., Kitamura, T., Miura, Y., Shimizu, T., *J Pediatr Endocrinol Metab* 2017, *30*, 939–946.

[135] Fernandez-Bravo, J., Andres, F. de, Zougagh, M., Rios, A., *J. Pharm. Biomed. Anal.* 2017, *145*, 40–45.

[136] Okuma, N., Saita, M., Hoshi, N., Soga, T., Tomita, M., Sugimoto, M., Kimoto, K., *PLoS One* 2017, *12*, e0183109.

[137] Macedo, A. N., Mathiaparanam, S., Brick, L., Keenan, K., Gonska, T., Pedder, L., Hill, S., Britz-McKibbin, P., *Acs Central Science* 2017, *3*, 904–913.

[138] Takahashi, H., Abe, H., Fujita, K., Sekine, K.-T., *Metabolomics* 2017, *13*, 51.

[139] Yoshida, K., Imamura, C. K., Hara, K., Mochizuki, M., Tanigawara, Y., *Metabolomics* 2017, *13*, 98.

[140] Sugiura, Y., Katsumata, Y., Sano, M., Honda, K., Kajimura, M., Fukuda, K., Suematsu, M., *Sci. Rep.* 2016, *6*, 32361.

[141] Suda, M., Shimizu, I., Yoshida, Y., Hayashi, Y., Ikegami, R., Katsuumi, G., Wakasugi, T., Yoshida, Y., Okuda, S., Soga, T., Minamino, T., *PLoS One* 2017, *12*, e0182422.

© 2018 WILEY-VCH Verlag GmbH & Co. KGaA, Weinheim

[142] Gonzalez-Pena, D., Dudzik, D., Garcia, A., Ancos, B. de, Barbas, C., Sanchez-Moreno, C., *Int. J. Mol. Sci.* 2017, *18*, 267.

[143] Matsui, T., Omuro, H., Liu, Y.-F., Soya, M., Shima, T., McEwen, B. S., Soya, H., *Proc. Natl. Acad. Sci. U.S.A.* 2017, *114*, 6358–6363.

[144] Matsumoto, M., Ooga, T., Kibe, R., Aiba, Y., Koga, Y., Benno, Y., *PLoS One* 2017, *12*, e0169207.

[145] Yamada, S., Kamada, N., Amiya, T., Nakamoto, N., Nakaoka, T., Kimura, M., Saito, Y., Ejima, C., Kanai, T., Saito, H., *Bmc Gastroenterology* 2017, *17*, 136.

[146] Gao, P., Ji, M., Fang, X., Liu, Y., Yu, Z., Cao, Y., Sun, A., Zhao, L., Zhang, Y., *Anal. Biochem.* 2017, *537*, 1–7.

[147] Matsuura, Y., Yamashita, A., Zhao, Y., Iwakiri, T., Yamasaki, K., Sugita, C., Koshimoto, C., Kitamura, K., Kawai, K., Tamaki, N., Zhao, S., Kuge, Y., Asada, Y., *PLoS One* 2017, *12*, e0175976.

[148] Kawaharada, R., Nakamura, A., Takahashi, K., Kikuchi, H., Oshima, Y., Kubohara, Y., *Life Sciences* 2016, *155*, 56–62.

[149] Mishima, E., Fukuda, S., Mukawa, C., Yuri, A., Kanemitsu, Y., Matsumoto, Y., Akiyama, Y., Fukuda, N. N., Tsukamoto, H., Asaji, K., Shima, H., Kikuchi, K., Suzuki, C., Suzuki, T., Tomioka, Y., Soga, T., Ito, S., Abe, T., *Kidney Int.* 2017, *92*, 634–645.

[150] Iwagaki, Y., Sugawara, S., Huruya, Y., Sato, M., Wu, Q., E, S., Yamamoto, K., Tsuduki, T., *Biosci. Biotechnol. Biochem.* 2018, *82*, 709–715.

[151] Sanchez-Lopez, E., Marcos, A., Ambrosio, E., Luisa Marina, M., Crego, A. L., *J. Chromatogr. A* 2016, *1467*, 372–382.

[152] Uebanso, T., Kano, S., Yoshimoto, A., Naito, C., Shimohata, T., Mawatari, K., Takahashi, A., *Nutrients* 2017, *9*, 756.

[153] Tsuji, M., *R. Soc. Open. Sci.* 2016, *3*, 160106.

[154] Miyamoto, Y., Mukai, T., Matsuoka, M., Kai, M., Maeda, Y., Makino, M., *PLoS Negl. Trop. Dis.* 2016, *10*, e0004881.

[155] Ishikawa, Y., Miyagi, A., Haishima, Y., Ishikawa, T., Nagano, M., Yamaguchi, M., Hihara, Y., Kawai-Yamada, M., *J. Plant Physiol.* 2016, *205*, 105–112.

[156] Ohba, T., Uemura, K., Nabetani, H., *Biosci. Biotechnol. Biochem.* 2017, *81*, 724–734.

[157] Hirasawa, T., Saito, M., Yoshikawa, K., Furusawa, C., Shmizu, H., *Biotechnol. J.* 2018, 1700612.

[158] Masumoto, H., Matsuyama, S., *PLoS One* 2018, *13*, e0194942.

[159] Li, L., Zhao, J., Zhao, Y., Lu, X., Zhou, Z., Zhao, C., Xu, G., *Sci. Rep.* 2016, *6*, 37976.

[160] Miyagi, A., Kitano, S., Oono, Y., Hase, Y., Narumi, I., Yamaguchi, M., Uchimiya, H., Kawai-Yamada, M., *Plant Physiol. Biochem.* 2018, *122*, 40–45.

[161] Zhao, J., Li, L., Zhao, Y., Zhao, C., Chen, X., Liu, P., Zhou, H., Zhang, J., Hu, C., Chen, A., Liu, G., Peng, X., Lu, X., Xu, G., *Anal. Bioanal. Chem.* 2018, *410*, 839–851.

[162] Das, G., Patra, J. K., Lee, S.-Y., Kim, C., Park, J. G., Baek, K.-H., *PLoS One* 2017, *12*, e0181280.

[163] Cheng, J., Wang, L., Liu, W., Chen, D. D. Y., *Anal. Chem.* 2017, *89*, 1411–1415.

[164] Sato, M., Miyagi, A., Yoneyama, S., Gisusi, S., Tokuji, Y., Kawai-Yamada, M., *Biosci. Biotechnol. Biochem.* 2017, *81*, 2314–2322.

[165] Gonzalez-Ruiz, V., Gagnebin, Y., Drouin, N., Codesido, S., Rudaz, S., Schappler, J., *Electrophoresis* 2018, *39*, 1222–1232.

[166] Mastrangelo, A., Panadero, M. I., Perez, L. M., Galvez, B. G., Garcia, A., Barbas, C., Ruperez, F. J., *Biochem. J.* 2016, *473*, 2187–2203.

[167] Barbas-Bernardos, C., Armitage, E. G., Garcia, A., Merida, S., Navea, A., Bosch-Morell, F., Barbas, C., *J. Pharm. Biomed. Anal.* 2016, *127*, 18–25.

[168] Ortiz-Villanueva, E., Benavente, F., Pina, B., Sanz-Nebot, V., Tauler, R., Jaumot, J., *Anal. Chim. Acta* 2017, *978*, 10–23.

[169] Marakova, K., Piestansky, J., Zelinkova, Z., Mikus, P., *Molecules* 2017, *22*, 1973.

[170] Piest'ansky, J., Marakova, K., Galba, J., Kovac, A., Mikus, P., *J. Sep. Sci.* 2017, *40*, 2292–2303.

[171] Hernández-Mesa, M., Cruces-Blanco, C., García-Campaña, A. M., *Talanta* 2017, *163*, 111–120.

[172] Attimarad, M., Nagaraja, S. H., Aldhubiab, B. E., Nair, A. B., Venugopala, K. N., *Indian Journal of Pharmaceutical Education and Research* 2017, *51*, 636–643.

[173] Švidrnoch, M., Boranova, B., Tomkova, J., Ondra, P., Maier, V., *Talanta* 2018, *176*, 69–76.

[174] dos Santos, V. B., Daniel, D., Singh, M., do Lago, C. L., *J. Chromatogr. B Analyt. Technol. Biomed. Life Sci.* 2016, *1038*, 19–25.

[175] DiBattista, A., Rampersaud, D., Lee, H., Kim, M., Britz-McKibbin, P., *Anal. Chem.* 2017, *89*, 11853–11861.

[176] Marakova, K., Piest'ansky, J., Mikus, P., *Chromatographia* 2017, *80*, 537–546.

[177] Schejbal, J., Slezackova, L., Reminek, R., Glatz, Z., *J. Chromatogr. A* 2017, *1487*, 235–241.

[178] Rollman, C. M., Moini, M., *Rapid Commun. Mass Spectrom.* 2016, *30*, 2070–2076.

[179] Holtkamp, H. U., Movassaghi, S., Morrow, S. J., Kubanik, M., Hartinger, C. G., *Metallomics* 2018, *10*, 455–462.

[180] Artner, C., Holtkamp, H. U., Kandioller, W., Hartinger, C. G., Meier-Menches, S. M., Keppler, B. K., *Chem. Commun. (Camb)* 2017, *53*, 8002–8005.

[181] Artner, C., Holtkamp, H. U., Hartinger, C. G., Meier-Menches, S. M., *J. Inorg. Biochem.* 2017, *177*, 322–327.

[182] Bytzek, A. K., Koellensperger, G., Keppler, B. K., G Hartinger, C., *J. Inorg. Biochem.* 2016, *160*, 250–255.

[183] Aleksenko, S. S., *J. Anal. Chem.* 2016, *71*, 711–716.

[184] Tascon, M., Gagliardi, L. G., Benavente, F., *Anal. Chim. Acta* 2017, *954*, 60–67.

[185] Liu, Y., Zhou, W., Mao, Z., Liao, X., Chen, Z., *J. Sep. Sci.* 2017, *40*, 4628–4635.

[186] Daniel, D., Lopes, F. S., dos Santos, V. B., do Lago, C. L., *Food. Chem.* 2018, *243*, 305–310.

© 2018 WILEY-VCH Verlag GmbH & Co. KGaA, Weinheim

[187] Kerrin, E. S., White, R. L., Quilliam, M. A., *Anal. Bioanal. Chem.* 2017, *409*, 1481–1491.

[188] Moreno-Gonzalez, D., Hamed, A. M., Gilbert-Lopez, B., Gamiz-Gracia, L., Garcia-Campana, A. M., *J. Chromatogr. A* 2017, *1510*, 100–107.

[189] Tejada-Casado, C., Moreno-Gonzalez, D., Lara, F. J., Garcia-Campana, A. M., del Olmo-Iruela, M., *J. Chromatogr. A* 2017, *1490*, 212–219.

[190] Lee, J.-H., Kim, S.-J., Lee, S., Rhee, J.-K., Lee, S. Y., Na, Y.-C., *Anal. Chim. Acta* 2017, *984*, 223–231.

[191] Ruzik, L., Kwiatkowski, P., *Talanta* 2018, *183*, 102–107.

[192] He, Y., Mo, F., Chen, D., Xu, L., Wu, Y., Fu, F., *Electrophoresis* 2017, *38*, 469–476.

[193] Mala, Z., Gebauer, P., *J. Chromatogr. A* 2017, *1518*, 97–103.

[194] Mala, Z., Gebauer, P., Bocek, P., *Anal. Chim. Acta* 2016, *935*, 249–257.

[195] Zhang, X.-H., Deng, Y., Zhao, M.-Z., Zhou, Y.-L., Zhang, X.-X., *RSC Advances* 2018, *8*, 4063–4071.

[196] Warren, C. R., *Soil Biol .Biochem.* 2016, *98*, 54–63.

[197] Warren, C. R., *Soil Biol. Biochem.* 2017, *110*, 44–55.

[198] Warren, C. R., *Soil Biol. Biochem.* 2017, *115*, 197–212.

[199] MacLennan, M. S., Tie, C., Kovalchik, K., Peru, K. M., Zhang, X., Headley, J. V., Chen, D. D. Y., *J. Environ. Sci.* 2016, *49*, 203–212.

[200] MacLennan, M. S., Peru, K. M., Swyngedouw, C., Fleming, I., Chen, D. D. Y., Headley, J. V., *Rapid Commun. Mass Spectrom.* 2018, *32*, 695–702.

[201] Tasi, A., Gaona, X., Fellhauer, D., Böttle, M., Rothe, J., Dardenne, K., Schild, D., Grivé, M., Colàs, E., Bruno, J., Källström, K., Altmaier, M., Geckeis, H., *Radiochimica Acta* 2018, *106*, 259–279.

[202] Kautenburger, R., Sander, J. M., Hein, C., *Electrophoresis* 2017, *38*, 930–937.

[203] Hahn, R., Hein, C., Sander, J. M., Kautenburger, R., *Appl. Geochem.* 2017, *78*, 241–249.

[204] Huynh, T.-N. S., Vidaud, C., Hagège, A., *Metallomics* 2016, *8*, 1185–1192.

[205] Sauge-Merle, S., Lemaire, D., Evans, R. W., Berthomieu, C., Aupiais, J., *Dalton Trans.* 2017, *46*, 1389–1396.

[206] Franze, B., Strenge, I., Engelhard, C., *J. Anal. At. Spectrom.* 2017, *32*, 1481–1489.

[207] Mozhayeva, D., Strenge, I., Engelhard, C., *Anal. Chem.* 2017, *89*, 7152–7159.

[208] Mozhayeva, D., Engelhard, C., *Anal Chem.* 2017, *89*, 9767–9774.

[209] Qu, H., Linder, S. W., Mudalige, T. K., *Anal. Bioanal. Chem.* 2017, *409*, 979–988.

[210] Matczuk, M., Legat, J., Shtykov, S. N., Jarosz, M., Timerbaev, A. R., *Electrophoresis* 2016, *37*, 2257–2259.

[211] Matczuk, M., Legat, J., Scaletti, F., Messori, L., Timerbaev, A. R., Jarosz, M., *J. Chromatogr. A* 2017, *1499*, 222–225.

[212] Legat, J., Matczuk, M., Timerbaev, A., Jarosz, M., *Chromatographia* 2017, *80*, 1695–1700.

[213] Legat, J., Matczuk, M., Timerbaev, A. R., Jarosz, M., *Anal. Bioanal. Chem.* 2018, *410*, 1151–1156.

[214] Hu, P., Zhang, W., Xin, H., Deng, G., *Front Cell Dev. Biol.* 2016, *4*, 116.

[215] Vera, M., Biswas, J., Senecal, A., Singer, R. H., Park, H. Y., *Annu. Rev. Genet.* 2016, *50*, 267–291.

[216] Zhang, L., Vertes, A., *Angew. Chem. Int. Ed. Engl.* 2018, *57*, 4466–4477.

[217] Onjiko, R. M., Morris, S. E., Moody, S. A., Nemes, P., *Analyst* 2016, *141*, 3648–3656.

[218] Lombard-Banek, C., Reddy, S., Moody, S. A., Nemes, P., *Mol. Cell Proteomics* 2016, *15*, 2756–2768.

[219] Onjiko, R. M., Portero, E. P., Moody, S. A., Nemes, P., *Anal. Chem.* 2017, *89*, 7069–7076.

[220] Khatri, K., Klein, J. A., Haserick, J. R., Leon, D. R., Costello, C. E., McComb, M. E., Zaia, J., *Anal. Chem.* 2017, *89*, 6645–6655.

[221] Itoi, T., Sugimoto, M., Umeda, J., Sofuni, A., Tsuchiya, T., Tsuji, S., Tanaka, R., Tonozuka, R., Honjo, M., Moriyasu, F., Kasuya, K., Nagakawa, Y., Abe, Y., Takano, K., Kawachi, S., Shimazu, M., Soga, T., Tomita, M., Sunamura, M., *Int. J. Mol. Sci.* 2017, *18*.

[222] Magalhães, P., Pontillo, C., Pejchinovski, M., Siwy, J., Krochmal, M., Makridakis, M., Carrick, E., Klein, J., Mullen, W., Jankowski, J., Vlahou, A., Mischak, H., Schanstra, J. P., Zürbig, P., Pape, L., *Proteomics Clin. Appl.* 2018, e1700163.

[223] Torati, L. S., Migaud, H., Doherty, M. K., Siwy, J., Mullen, W., Mesquita, P. E. C., Albalat, A., *PLoS One* 2017, *12*, e0186692.

[224] Nkuipou-Kenfack, E., Schanstra, J. P., Bajwa, S., Pejchinovski, M., Vinel, C., Dray, C., Valet, P., Bascands, J.-L., Vlahou, A., Koeck, T., Borries, M., Busch, H., Bechtel-Walz, W., Huber, T. B., Rudolph, K. L., Pich, A., Mischak, H., Zürbig, P., *PLoS One* 2017, *12*, e0166875.

[225] Mary, S., Small, H. Y., Siwy, J., Mullen, W., Giri, A., Delles, C., *Hypertension* 2017, *69*, 910–918.

[226] Weissinger, E. M., Human, C., Metzger, J., Hambach, L., Wolf, D., Greinix, H. T., Dickinson, A. M., Mullen, W., Jonigk, D., Kuzmina, Z., Kreipe, H., Schweier, P., Böhm, O., Türüchanow, I., Ihlenburg-Schwarz, D., Raad, J., Durban, A., Schiemann, M., Könecke, C., Diedrich, H., Holler, E., Beutel, G., Krauter, J., Ganser, A., Stadler, M., *Leukemia* 2017, *31*, 654–662.

[227] Sotgia, S., Mangoni, A. A., Forteschi, M., Murphy, R. B., Elliot, D., Sotgiu, E., Pintus, G., Carru, C., Zinellu, A., *Molecules* 2016, *21*, 1298.

[228] Zhang, S., Raedschelders, K., Santos, M., van Eyk, J. E., *J. Proteome Res.* 2017, *16*, 4515–4522.

[229] Park, S.-J., Lee, S. A., Prasain, N., Bae, D., Kang, H., Ha, T., Kim, J. S., Hong, K.-S., Mantel, C., Moon, S.-H., Broxmeyer, H. E., Lee, M. R., *Stem Cells Dev.* 2017, *26*, 734–742.

[230] Xu, W., Okayama, N., Iwasawa, A., Yayota, M., *Anim. Sci. J.* 2017, *88*, 1352–1363.

[231] Muroya, S., Oe, M., Ojima, K., *Meat Sci.* 2018, *137*, 228–234.

[232] Hatakeyama, H., Fujiwara, T., Sato, H., Terui, A., Hisaka, A., *Biol. Pharm. Bull.* 2018, *41*, 619–627.

© 2018 WILEY-VCH Verlag GmbH & Co. KGaA, Weinheim

[233] Kajihara, N., Kukidome, D., Sada, K., Motoshima, H., Furukawa, N., Matsumura, T., Nishikawa, T., Araki, E., *J. Diabetes Investig.* 2017, *8*, 750–761.

[234] Takahashi, Y., Tamura, Y., Matsunaga, Y., Kitaoka, Y., Terada, S., Hatta, H., *J. Nutr. Sci. Vitaminol. (Tokyo)* 2016, *62*, 257–264.

[235] Toyoda, Y., Kashikura, K., Soga, T., Tagawa, Y.-i., *J. Toxicol. Sci.* 2017, *42*, 445–454.

[236] Fukai, K., Harada, S., Iida, M., Kurihara, A., Takeuchi, A., Kuwabara, K., Sugiyama, D., Okamura, T., Akiyama, M., Nishiwaki, Y., Oguma, Y., Suzuki, A., Suzuki, C., Hirayama, A., Sugimoto, M., Soga, T., Tomita, M., Takebayashi, T., *PLoS One* 2016, *11*.

[237] Miyagi, A., Uchimiya, H., Kawai-Yamada, M., *Food Chem.* 2017, *218*, 561–568.

[238] Burgos, R. C. R., Cervinkova, K., van der Laan, T., Ramautar, R., van Wijk, E. P. A., Cifra, M., Koval, S., Berger, R., Hankemeier, T., van der Greef, J., *J. Photochem. Photobiol. B* 2016, *163*, 237–245.

[239] Burgos, R. C. R., Zhang, W., van Wijk, E. P. A., Hankemeier, T., Ramautar, R., van der Greef, J., *J. Photochem. Photobiol. B, Biol.* 2017, *175*, 291–296.

[240] Acket, S., Degournay, A., Gosset, M., Merlier, F., Troncoso-Ponce, M. A., Thomasset, B., *Anal. Biochem.* 2018, *547*, 14–18.

[241] Frohnhöfer, H. G., Geiger-Rudolph, S., Pattky, M., Meixner, M., Huhn, C., Maischein, H.-M., Geisler, R., Gehring, I., Maderspacher, F., Nüsslein-Volhard, C., Irion, U., *Biology Open* 2016, *5*, 736–744.

[242] Foteeva, L. S., Matczuk, M., Pawlak, K., Aleksenko, S. S., Nosenko, S. V., Karandashev, V. K., Jarosz, M., Timerbaev, A. R., *Anal. Bioanal. Chem.* 2017, *409*, 2421–2427.

[243] Aupiais, J., Younes, A., Moisy, P., Hennig, C., Rossberg, A., Brunel, B., Kerbaa, M., Vidaud, C., Den Auwer, C., *New J. Chem.* 2017, *41*, 11291–11298.

[244] Izu, H., Shigemori, K., Eguchi, M., Kawane, S., Fujii, S., Kitamura, Y., Aoshima, H., Yamada, Y., *Food Chem.* 2017, *214*, 354–359.

[245] Mateos-Vivas, M., Dominguez-Alvarez, J., Rodriguez-Gonzalo, E., Carabias-Martinez, R., *Food Chem.* 2017, *233*, 38–44.

[246] Ivanova-Petropulos, V., Nace Va, Z., Sand Or, V., Maksz In, L., Na Gy, L., Berki Cs, B., Stafilov, T., Kilar, F., *Electrophoresis* 2018, *39*, 1597–1605.

[247] Li, J-X., Sun, C-J., Zheng, L., Jiang, F-H., Yin, X-F., Chen, J-H., Wang, X-R., *Chinese J. Analytical Chem.* 2016, *44*, 1659–1664.

[248] Jiang, W., Jin, X., Yu, X., Wu, W., Xu, L., Fu, F., *J. Chromatogr. A* 2017, *1496*, 167–173.

© 2018 WILEY-VCH Verlag GmbH & Co. KGaA, Weinheim